Type-1.5 superconductivity in multiband systems: Effects of interband couplings

Johan Carlström,[1] Egor Babaev,[1,2] and Martin Speight[3]
[1]*Department of Theoretical Physics, The Royal Institute of Technology, Stockholm S-10691 Sweden*
[2]*Department of Physics, University of Massachusetts, Amherst, Massachusetts 01003, USA*
[3]*School of Mathematics, University of Leeds, Leeds LS2 9JT, United Kingdom*
(Received 16 September 2010; revised manuscript received 19 March 2011; published 11 May 2011)

In contrast to single-component superconductors, which are described at the level of Ginzburg-Landau theory by a single parameter κ and are divided in type-I $\kappa < 1/\sqrt{2}$ and type-II $\kappa > 1/\sqrt{2}$ classes, two-component systems in general possess three fundamental length scales and have been shown to possess a separate "type-1.5" superconducting state. In that state, as a consequence of the extra fundamental length scale, vortices attract one another at long range but repel at shorter ranges, and therefore should form clusters in low magnetic fields. In this work we investigate the appearance of type-1.5 superconductivity and the interpretation of the fundamental length scales in the case of two active bands with substantial interband couplings such as intrinsic Josephson coupling, mixed gradient coupling, and density-density interactions. We show that in the presence of substantial intercomponent interactions of the above types the system supports type-1.5 superconductivity with fundamental length scales being associated with the mass of the gauge field and two masses of normal modes represented by *mixed* combinations of the density fields.

DOI: 10.1103/PhysRevB.83.174509 PACS number(s): 74.25.Uv, 74.25.Ha, 74.25.Op, 74.20.De

I. INTRODUCTION

According to Ginzburg-Landau theory, a conventional superconductor near T_c is described by a single complex order-parameter field. The physics of these systems is governed by two fundamental length scales, the magnetic-field penetration depth λ and the coherence length ξ, and the ratio κ of these determines the response to an external field, sorting them into two categories as follows: type I when $\kappa < 1/\sqrt{2}$ and type II when $\kappa > 1/\sqrt{2}$.[1]

Type-I superconductors expel weak magnetic fields, while strong fields give rise to formation of macroscopic normal domains with magnetic flux.[2] The response of type-II superconductors is completely different; below some critical value H_{c1}, the field is expelled. Above this value a superconductor forms a lattice or a liquid of vortices that have a supercurrent circulating around a normal core and carry magnetic flux through the system. Finally, at a higher second critical value, H_{c2} superconductivity is destroyed.

These different responses are usually viewed as consequences of the vortex interaction in these systems, the energy cost of a boundary between superconducting and normal states and the thermodynamic stability of vortex excitations. In a type-II superconductor the energy cost of a boundary between the normal and the superconducting state is negative, while the interaction between vortices is repulsive.[1] This leads to a formation of stable vortex lattices and liquids. In type-I superconductors the situation is the opposite; the vortex interaction is attractive (thus making them unstable against collapse into one large vortex), while the boundary energy between normal and superconducting states is positive. From a thermodynamic point of view the principal difference between type-I and type-II states is the following: (i) In type-II superconductors the external magnetic-field strength required to make formation of vortex excitations energetically preferred, H_{c1}, is smaller than the thermodynamical magnetic field H_{ct} (the field whose energy density is equal to the condensation energy of a superconductor, i.e., the field at which the uniform superconducting state becomes thermodynamically unstable). (ii) In type-I superconductors the field strength required to create a vortex excitation is larger than the thermodynamical critical magnetic field, i.e., vortices cannot form. One can distinguish also a special "zero measure" boundary case where κ has a critical value exactly at the type-I–type-II boundary, which in the most common Ginzburg-Landau (GL) model parametrization corresponds to $\kappa = 1/\sqrt{2}$. In that case vortices do not interact[3] in the Ginzburg-Landau theory.

The above circumstances result in a situation where, in a strong external magnetic field, type-I superconductors usually have a tendency to minimize boundary energy between the normal and superconducting states, leading to a formation of large inclusions of normal phase which frequently have laminar structure.[2]

Recently there has been increased interest in superconductors with several superconducting components. The main situations where multiple superconducting components arise are (i) multiband superconductors,[4–9] (ii) mixtures of independently conserved condensates such as the projected superconductivity in metallic hydrogen and hydrogen rich alloys,[10–12] and (iii) superconductors with other than *s*-wave pairing symmetries. In this work we focus on cases (i) and (ii). The principal difference between cases (i) and (ii) is the absence of the intercomponent Josephson coupling in case (ii).

In two-band superconductors (i) the superconducting components originate from electronic Cooper pairing in different bands.[4] Therefore these condensates could not *a priori* be expected to be independently conserved. This, at the level of effective models, should manifest itself in a rather generic presence of intercomponent Josephson coupling.

In case (ii) two superconducting components were predicted to originate from electronic and protonic Cooper pairing in metallic hydrogen or hydrogen-rich alloys. In the projected liquid metallic deuterium or deuterium-rich alloys, electronic superconductivity was predicted to coexist at ultrahigh pressures with deuteronic Bose-Einstein condensation

condensation.[10–12] Because electrons cannot be converted to protons or deuterons the condensates are independently conserved, and therefore in the effective model intercomponent Josephson coupling is forbidden on symmetry grounds. These states are currently a subject of a renewed experimental pursuit. They are expected to arise at high but experimentally accessible pressures (≈400 GPa). Current static compression experiments achieve pressures of ≈350 GPa with pressures of an order of 1 TPa being anticipated in diamond-anvil cell experiments due to the recent availability of ultrahard diamonds. Similar two-charged component models were discussed in the context of the physics of neutron stars where they represent coexistent protonic and Σ^--hyperon Cooper pairs in the neutron star interior.[13]

This wide variety of systems raises the need to understand and classify the possible magnetic responses of multicomponent superconductors. It was discussed recently that in multicomponent systems the magnetic response is much more complex than in ordinary systems, and that the type-I/type-II dichotomy is not sufficient for classification. Rather, in a wide range of parameters, as a consequence of the existence of three fundamental length scales, there is a separate superconducting regime where vortices have long-range attractive, short-range repulsive interaction and form vortex clusters immersed in domains of the two-component Meissner state.[14,15] Recent experimental works[16,17] have put forward the suggestion that this state is realized in the two-band material MgB_2, which sparked growing interest in this topic. In particular, questions were raised over whether this "type-1.5" superconducting regime (as it was termed by Moshchalkov *et al.*[16] for recent works, see Ref. 18) is possible even in principle in the case of various nonvanishing couplings (e.g., intrinsic Josephson coupling, mixed gradient couplings, etc.) between superconducting components in different bands.

In this work we report a study of the appearance of type-1.5 superconductivity especially focusing on the case of multiband superconductivity, demonstrating the persistence of this type of superconductivity in the presence of various kinds of intercomponent couplings (such as interband Josephson coupling, mixed gradient coupling, and density-density and other kinds of couplings).

A. Type-1.5 superconductivity

The possibility of a new type of superconductivity, distinct from the type I and type II in multicomponent systems,[14,15] is based on the following considerations. In principle the boundary problem in the Ginzburg-Landau type of equations in the presence of phase winding is *not*, from a rigorous point of view, reducible to a one-dimensional problem in general. Furthermore, as discussed in Refs. 14 and 15, in general in two-component models there are *three fundamental length scales*, which renders the model impossible to parametrize in terms of a single dimensionless parameter κ. In the case where the condensates are not coupled by interband Josephson coupling but only by the vector potential these length scales are the two independent coherence lengths of the condensates (set by the inverse masses of the corresponding scalar density fields) and magnetic-field penetration length (set by the inverse mass acquired by the gauge field). In contrast, in the case

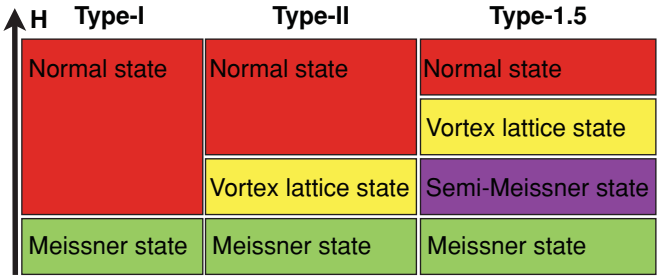

FIG. 1. (Color online) A comparison of the magnetic phase diagrams of clean bulk type-I, type-II, and type-1.5 superconductors at zero temperature. The semi-Meissner state is a macroscopic phase separation into a two-component Meissner state and vortex clusters where one of the density modes is suppressed by core overlaps.

where the condensates are coupled by interband Josephson terms, one cannot distinguish independent coherence lengths attributed to different condensates. Nonetheless, in this case the density variations can also possess two fundamental length scales,[15] in contrast to single-component theories. We elaborate on this fact below. In Refs. 14 and 15 vortex solutions in two-component theories were found that have nonmonotonic vortex interaction, with a long-range attractive part determined by a dominant density-density interaction and a short-range repulsive part produced by current-current and electromagnetic interactions. An important circumstance that was demonstrated was that these vortices are thermodynamically stable in spite of the existence of the attractive tail in the interaction.

A non-monotonic intervortex interaction potential should result in the formation of vortex clusters in low magnetic field immersed into the vortexless areas, a state referred to in Ref. 14 as the "semi-Meissner state." Figure 1 shows the schematic phase diagram of a type-1.5 superconductor.

If the vortices form clusters one cannot use the usual one-dimensional argument concerning the energy of superconductor-to-normal state boundary to classify the magnetic response of the system. First of all, the energy per vortex in such a case depends on whether a vortex is placed in a cluster or not: i.e., formation of a single isolated vortex might be energetically unfavorable, while formation of vortex clusters is favorable, because in a cluster where vortices are placed in a minimum of the interaction potential, the energy per flux quantum is smaller than that for an isolated vortex (thermodynamically the nonmonotonic two-vortex interaction potential predicts that the smallest energy per flux quantum will be in the case of a uniform lattice with spacing equal to the minimum of two-body intervortex potential).

Thus besides the energy of a vortex in a cluster, there appears an additional energy characteristic associated with the boundary of a cluster. In other words, in this situation, to determine the magnetic response of a system it is not sufficient to study the one-dimensional boundary problem nor the single-vortex problem, in contrast to single-component systems. Moreover, in a cluster the system tends to minimize the boundary energy of a cluster (similarly to type-I behavior), while breaking into a lattice of one-quantum vortices inside the cluster (similarly to type-II systems with negative interface energy). Thus, in an increased magnetic field the vortices

TABLE I. Basic characteristic of bulk clean superconductors in type-I, type-II and type-1.5 regimes. Here the most common units are used in which the value of the GL parameter $\kappa = \lambda/\xi$ which separates type-I and type-II regimes is $\kappa_c = 1/\sqrt{2}$.

	Single-component type I	**Single-component type II**	**Multicomponent type 1.5**
Characteristic lengths scales	Penetration length λ and coherence length ξ ($\frac{\lambda}{\xi} < \frac{1}{\sqrt{2}}$)	Penetration length λ and coherence length ξ ($\frac{\lambda}{\xi} > \frac{1}{\sqrt{2}}$)	Two characteristic density variations length scales ξ_1,ξ_2 and penetration length λ, the nonmonotonic vortex interaction occurs in these systems typically when $\xi_1 < \sqrt{2}\lambda < \xi_2$
Intervortex interaction	Attractive	Repulsive	Attractive at long range and repulsive at short range
Energy of superconducting/ normal-state boundary	Positive	Negative	Under quite general conditions negative energy of superconductor/ normal interface inside a vortex cluster but positive energy of the vortex cluster's boundary
The magnetic field required to form a vortex	Larger than the thermodynamical critical magnetic field	Smaller than thermodynamical critical magnetic field	In different cases either (i) smaller than the thermodynamical critical magnetic field or (ii) larger than critical magnetic field for a single vortex but smaller than the critical magnetic field for a vortex cluster of a certain critical size
Phases in external magnetic field	(i) Meissner state at low fields (ii) Macroscopically large normal domains at larger fields. First order phase transition between superconducting and normal states	(i) Meissner state at low fields (ii) Vortex lattices/liquids at larger fields. Second order phase transitions between superconducting and vortex states and between vortex and normal states	(i) Meissner state at low fields (ii) "Semi-Meissner state": vortex clusters coexisting with Meissner domains at intermediate fields (iii) Vortex lattices/ liquids at larger fields. Vortices form via a first order phase transition. The transition from vortex states to normal state is second order.
Energy $E(N)$ of N-quantum axially symmetric vortex solutions	$\frac{E(N)}{N} < \frac{E(N-1)}{N-1}$ for all N. Vortices coalesce onto a single N-quantum megavortex	$\frac{E(N)}{N} > \frac{E(N-1)}{N-1}$ for all N. N-quantum vortex decays into N infinitely separated single-quantum vortices quantum vortices	There is a characteristic number N_c such that $\frac{E(N)}{N} < \frac{E(N-1)}{N-1}$ for $N < N_c$, while $\frac{E(N)}{N} > \frac{E(N-1)}{N-1}$ for $N > N_c$. N-quantum vortices decay into vortex clusters.

forms via a first order phase transition. A magnetic phase distinct from the vortex and Meissner states, which then arises, is a macroscopic phase separation into domains of a two-component Meissner state and vortex clusters where one of the density modes is suppressed by core overlap. We summarize the basic properties of type-I, type-II, and type-1.5 regimes in Table I.

The existence of thermodynamically stable type-1.5 superconducting regimes ultimately depends on the existence of a nonmonotonic intervortex interaction potential. It is an important question how generic this effect is. In this work we mainly focus on multiband realizations of multicomponent superconductivity and investigate the effects of interband Josephson coupling, mixed gradient coupling, and density-density coupling terms on vortex interactions in two-band superconductors. We show that (i) when these and other similar kinds of couplings are present, the system still can possess three fundamental length scales, in contrast to the two length scales in the usual single-component GL theory, and (ii) nonmonotonic interaction potential resulting from these scales is possible in a wide parameter range in these models.

The structure of this paper is as follows: In Sec. II we introduce the model. In Sec. III we present a linear theory of asymptotics of the vortex fields in a superconductor with two bands with various interband couplings. We begin Sec. III by demonstrating that for a *general* form of the effective potential in a two-band (or more generally two-gap) Ginzburg-Landau free energy, the linear theory gives, under quite general conditions, two fundamental length scales of the variations of the densities. From the linearized theory we calculate the long-range intervortex interaction potentials using the two-component generalization of the point-vortex method[19] and show how the nonmonotonic intervortex interaction potential arises from the interplay of two fundamental length scales

of the superfluid density variations and the magnetic-field penetration length. The central point of this part is how the fundamental length scales are defined in the presence of interband coupling as well as the occurrence of "mode mixing." Next we move to quantitatively study the effects of several kinds of intercomponent couplings which quite generically arise in two-component theories. In Sec. III D we demonstrate that mixed gradient coupling can lead, under certain conditions, to an *increase* in the disparity of the characteristic scales of the density variations. In Sec. IV we present a large scale numerical study of the full nonlinear problem of the interaction between a pair of vortices.

II. MODEL

A. Free-energy functional

We study the type-1.5 regime using the following two-component Ginzburg-Landau (TCGL) free-energy functional,

$$F = \tfrac{1}{2}(D\psi_1)(D\psi_1)^* + \tfrac{1}{2}(D\psi_2)(D\psi_2)^* - \nu \mathrm{Re}\{(D\psi_1)(D\psi_2)^*\} + \tfrac{1}{2}(\nabla\times\mathbf{A})^2 + F_p. \quad (1)$$

Here $D = \nabla + ie\mathbf{A}$, and $\psi_a = |\psi_a| e^{i\theta_a}$, $a = 1,2$, represent two superfluid components which, in a two-band superconductor, correspond to two superfluid densities in different bands. The term F_p can contain in our analysis an *arbitrary* collection of nongradient terms.

A particular form of two-component GL model, which was microscopically derived in Refs. 6–8 for two-band superconductors is

$$F = \tfrac{1}{2}(D\psi_1)(D\psi_1)^* + \tfrac{1}{2}(D\psi_2)(D\psi_2)^* - \nu \mathrm{Re}\{(D\psi_1)(D\psi_2)^*\} + \tfrac{1}{2}(\nabla\times\mathbf{A})^2 + \alpha_1|\psi_1|^2 + \tfrac{1}{2}\beta_1|\psi_1|^4 + \alpha_2|\psi_2|^2 + \tfrac{1}{2}\beta_2|\psi_2|^4 - \eta_1|\psi_1||\psi_2|\cos(\theta_1-\theta_2) + \eta_2|\psi_1|^2|\psi_2|^2. \quad (2)$$

The first two terms represent standard Ginzburg-Landau gradient terms, the second term represents mixed gradient interactions, which were shown to originate in two-band superconductors from impurity scattering.[6,7] The next term is the magnetic-field energy density and the remaining terms represent an effective potential. Here we note that α_1 and α_2 can invert sign at different temperatures. The regime where α_1 is positive while α_2 is negative corresponds to the situation where one of the bands has no superconductivity of its own but nonetheless bears some superfluid density due to interband Josephson tunneling, which is represented here by the term $\eta_1|\psi_1||\psi_2|\cos(\theta_1-\theta_2)$. The type-1.5 behavior in this regime was studied in Ref. 15. In this work we will mainly focus on the situation where both bands are active, i.e., $\alpha_{1,2} < 0$. For generality we also add a higher-order density-density coupling term $\eta_2|\psi_1|^2|\psi_2|^2$. We also consider the case of independently conserved condensates where the third and ninth terms in Eq. (2) are forbidden on symmetry grounds, that is, $\nu = \eta_1 = 0$ (see also remark, Ref. 20). The equivalence mapping between our units and the standard textbook units is given in Appendix V.

A microscopic derivation of the TCGL model (2) requires the fields $|\psi_a|$ to be small. However, it does not in principle require α_a to change sign at the same temperature. Moreover, as in the case of single-component GL theory, we expect model (2) to give in many cases a qualitatively acceptable picture in lower temperature regimes as well. In fact, our analysis can in some cases give a qualitative picture for the case where one of the fields does not possess a GL-type effective potential because the regime where one of the bands is in a London limit (i.e., it does not possess a GL effective potential but has a small vortex core modeled by a sharp cutoff) can be recovered from our analysis as a limiting case. As will be clear from the analysis below, that regime also supports type-1.5 superconductivity.

B. Basic properties of the vortex excitations

The only vortex solutions of model (2) that have finite energy per unit length are the integer N-flux quantum vortices, which have the following phase windings along a contour l around the vortex core: $\oint_l \nabla\theta_1 = 2\pi N$, $\oint_l \nabla\theta_2 = 2\pi N$. Vortices with differing phase windings carry a fractional multiple of the magnetic-flux quantum and have energy divergent with the system size. These solutions were investigated in detail in Ref. 21. In what follows we investigate only integer flux vortex solutions, which are the energetically cheapest objects to produce by means of an external field in a bulk superconductor.

III. VORTEX ASYMPTOTICS

The key to understanding the interaction of well separated vortices is to analyze the large r asymptotics of the vortex solution. We will analyze this problem in the context of a general TCGL model whose free energy takes the form

$$F = \tfrac{1}{2}(D_i\psi_1)^* D_i\psi_1 + \tfrac{1}{2}(D_i\psi_2)^* D_i\psi_2 + \tfrac{1}{2}(\partial_1 A_2 - \partial_2 A_2)^2 + F_p, \quad (3)$$

where F_p contains all the nongradient terms (in particular, but not restricted to, Josephson and density-density interaction terms). This free energy is consistent with Eq. (2) in the case $\nu = 0$. We will show in Sec. III D how to handle mixed gradient terms. *The precise form of F_p is not crucial for our analysis in this section.* By gauge invariance, it can depend on the condensates only via $|\psi_1|$, $|\psi_2|$ and (if the condensates are not independently conserved) on $\theta_1 - \theta_2$. We will assume that F_p takes its minimum value (which we normalize to be 0) when $|\psi_1| = u_1 > 0$, $|\psi_2| = u_2 > 0$, and $\theta_1 - \theta_2 = 0$. So, either there is no phase coupling (F_p is independent of $\theta_1 - \theta_2$) and the choice of $\theta_1 - \theta_2 = 0$ is arbitrary, or the phase coupling is such as to encourage phase locking. (Note that the case of phase antilocked fields can trivially be recovered from our analysis by mapping $\psi_2 \mapsto -\psi_2$.)

The field equations are obtained from F by demanding that the total free energy $E = \int F dx_1 dx_2$ is stationary with respect to all variations of ψ_1, ψ_2, and A_i. A routine calculation yields

$$D_i D_i \psi_a = 2\frac{\partial F_p}{\partial \psi_a^*}, \quad (4)$$

$$\partial_i(\partial_i A_j - \partial_j A_i) = e\sum_{a=1}^{2} \mathrm{Im}(\psi_a^* D_j \psi_a). \quad (5)$$

This triple of coupled nonlinear partial differential equations supports solutions of the form

$$\psi_a = f_a(r)e^{i\theta}, \quad (A_1, A_2) = \frac{a(r)}{r}(-\sin\theta, \cos\theta), \tag{6}$$

where f_1, f_2, a are real profile functions. Note that in some cases mixed gradient terms favor nonaxially symmetric solutions. In this section we consider only axially symmetric vortices. Fields within the above ansatz satisfy the field equations if and only if the profile functions $f_1(r), f_2(r), a(r)$ satisfy the coupled ordinary differential equation system

$$f_a'' + \frac{1}{r}f_a' - \frac{1}{r^2}(1+ea)^2 f_a = \left.\frac{\partial F_p}{\partial|\psi_a|}\right|_{(u_1,u_2,0)}, \tag{7}$$

$$a'' - \frac{1}{r}a' - e(1+ea)\left(f_1^2 + f_2^2\right) = 0. \tag{8}$$

The solution we require, the vortex, has boundary behavior $f_a(r) \to u_a$, $a(r) \to -1/e$ as $r \to \infty$. So, for large r, the quantities

$$\epsilon_a(r) = f_a(r) - u_a, \quad \alpha(r) = a(r) + \frac{1}{e} \tag{9}$$

are small and so should, to leading order, satisfy the *linearization* of Eqs. (7) and (8) about $(u_1, u_2, -1/e)$. That is, at large r,

$$\epsilon_a'' + \frac{1}{r}\epsilon_a' = \sum_{b=1}^{2} \mathcal{H}_{ab}\epsilon_b, \tag{10}$$

$$\alpha'' - \frac{1}{r}\alpha' - e^2\left(u_1^2 + u_2^2\right)\alpha = 0, \tag{11}$$

where $\mathcal{H}$ is the Hessian matrix of $F_p(|\psi_1|, |\psi_2|, 0)$ about its minimum

$$\mathcal{H}_{ab} = \left.\frac{\partial^2 F_p}{\partial|\psi_a|\partial|\psi_b|}\right|_{(u_1,u_2,0)}. \tag{12}$$

So α decouples from ϵ_1, ϵ_2 asymptotically, and we see immediately that

$$\alpha(r) = q_0 r K_1(\mu_A r), \quad \mu_A = e\sqrt{u_1^2 + u_2^2}, \tag{13}$$

where K_n denotes the nth modified Bessel's function of the second kind,[22] and q_0 is an unknown real constant. Hence at large r,

$$\boldsymbol{A} \sim \left(-\frac{1}{er} + q_0 K_1(\mu_A r)\right)(-\sin\theta, \cos\theta). \tag{14}$$

Since, for all n,

$$K_n(s) \sim \sqrt{\frac{\pi}{2s}}e^{-s} \quad \text{as} \quad s \to \infty, \tag{15}$$

it follows that the magnetic field decays exponentially as a function of r, with length scale (penetration depth)

$$\lambda \equiv \frac{1}{\mu_A} = \frac{1}{e\sqrt{u_1^2 + u_2^2}}. \tag{16}$$

By contrast, Eq. (10) represents, in general, a coupled pair of ordinary differential equations for ϵ_1, ϵ_2. Since $(u_1, u_2, 0)$ is a *minimum* of $F_p(|\psi_1|, |\psi_2|, \theta_1 - \theta_2)$, the Hessian matrix $\mathcal{H}$ is a *positive definite* symmetric 2×2 real matrix. Hence its eigenvalues, μ_1^2, μ_2^2 say, are real and positive, and its eigenvectors, v_1, v_2 say, form an orthonormal basis for $\mathbb{R}^2$. Expanding $\epsilon = (\epsilon_1, \epsilon_2)^T$ in the basis v_1, v_2,

$$\epsilon(r) = \chi_1(r)v_1 + \chi_2(r)v_2, \tag{17}$$

we see that χ_1, χ_2 satisfy the *uncoupled* pair of ordinary differential equations

$$\chi_a'' + \frac{1}{r}\chi_a' = \mu_a^2\chi_a, \tag{18}$$

whence

$$\chi_a(r) = q_a K_0(\mu_a r) \tag{19}$$

for some (unknown) constants q_1, q_2. Since v_1, v_2 are orthonormal, there is an angle Θ, which we call the *mixing angle*, such that the eigenvectors of $\mathcal{H}$ are

$$v_1 = \begin{pmatrix}\cos\Theta \\ \sin\Theta\end{pmatrix}, \quad v_2 = \begin{pmatrix}-\sin\Theta \\ \cos\Theta\end{pmatrix}. \tag{20}$$

Hence at large r the density fields behave as

$$\begin{aligned}\psi_1 &\sim [u_1 + q_1\cos\Theta K_0(\mu_1 r) - q_2\sin\Theta K_0(\mu_2 r)]e^{i\theta}, \\ \psi_2 &\sim [u_2 + q_1\sin\Theta K_0(\mu_1 r) + q_2\cos\Theta K_0(\mu_2 r)]e^{i\theta}.\end{aligned} \tag{21}$$

where, once again, K_0 is a Bessel function.

This analysis implies the following:

(1) In general there are three fundamental length scales in the problem (in contrast to the two length scales of one-component Ginzburg-Landau theory) which manifest themselves in the vortex asymptotics, namely $1/\mu_A$, $1/\mu_1$, and $1/\mu_2$.

(2) These are constructed from the vacuum expectation values u_a of $|\psi_a|$ (in the case of $1/\mu_A$) and from the eigenvalues of $\mathcal{H}$, the Hessian matrix of F_p about the vacuum (i.e., the ground state).

(3) $1/\mu_A$ can be interpreted as the London penetration length of the magnetic field.

(4) However, unless the mixing angle Θ is a multiple of $\pi/2$, $1/\mu_1$ and $1/\mu_2$ cannot be interpreted as the coherence lengths of ψ_1, ψ_2 in the usual sense. This is because the normal modes of the field theory close to the vacuum are not $|\psi_a| - u_a$, but rather

$$\begin{aligned}\chi_1 &= (|\psi_1| - u_1)\cos\Theta - (|\psi_2| - u_2)\sin\Theta, \\ \chi_2 &= (|\psi_1| - u_1)\sin\Theta - (|\psi_2| - u_2)\cos\Theta\end{aligned}$$

obtained by rotating through the mixing angle Θ, which is also determined by $\mathcal{H}$. Therefore in general (e.g., in the presence of intercomponent Josephson coupling) for a one-flux quantum axially symmetric vortex, the recovery of both fields ψ_a at *very* long range will be according to the same exponential law, set by the smaller of the masses μ_1, μ_2; one should use the representation in terms of the fields $\chi_{1,2}$ to handle properly the two length scales associated with the density recovery.

(5) This analysis tells us only about the vortex structure at large r. It gives no direct information on the vortex core, which is important to understand quantitatively the nature of the vortex interactions at intermediate and short distances. This will be studied numerically in Sec. V.

Since the gauge field mediates a repulsive force between vortices, while the condensate fields mediate an attractive

force, it is clear that we can read off from the above analysis the condition under which the intervortex force is attractive at long range: we require that $1/\mu_A$ is *not* the longest of the three length scales, or, more explicitly, that (at least) one of the eigenvalues of $\mathcal{H}$ should be less than $\mu_A^2 = e^2(u_1^2 + u_2^2)$. We can predict an explicit formula for the long-range two-vortex interaction potential, using the point vortex formalism[19] (a brief review of the method in given in Appendix V). This rests on the observation that, far from its core, the fields of the vortex are identical to those of a hypothetical point particle in a linear theory with two Klein-Gordon fields (χ_1 and χ_2 above) of mass μ_1,μ_2 and a vector field (A) of mass μ_A. The point particle carries scalar monopole charges $2\pi q_1$ and $2\pi q_2$ and a magnetic dipole moment $2\pi q_0$. Two such hypothetical particles held distance r apart would experience an interaction potential

$$V(r) = 2\pi\left[q_0^2 K_0(\mu_A r) - q_1^2 K_0(\mu_1 r) - q_2^2 K_0(\mu_2 r)\right]. \quad (22)$$

This formula reproduces the prediction explained above: the long-range interaction will be attractive if (at least) one of μ_1,μ_2 is less than μ_A.

One can ask, retrospectively, whether the approximation of *linearizing* in the small quantities $\alpha(r),\chi_1(r),\chi_2(r)$ is well justified. Rigorous analysis of the single-component model[23] shows that if either of the scalar mode masses, μ_2 say, exceeds $2\mu_A$, then quadratic terms in α become comparable at large r with linear terms in χ_2, so that the equation for χ_2 should include extra terms. In this case, χ_2 decays like $K_0(\mu_A r)^2$ rather than $K_0(\mu_2 r)$. One should note, however, that, unless $\mu_1 > 2\mu_A$ also, the *leading* term in Eq. (21), decaying like $K_0(\mu_1 r)$, is still correct, and it is only the leading term that determines the nature (attractive or repulsive) of the intervortex interactions at long range. The case of interest to us is when the long-range force is attractive, that is, when at least one of μ_1,μ_2 is *less than* μ_A, so the linearized analysis presented above suffices for our purposes.

A. U(1) × U(1) symmetric model

We first illustrate the above analysis in the case of U(1) × U(1) condensates coupled only by a gauge field[14] where

$$F_p = \alpha_1|\psi_1|^2 + \frac{\beta_1}{2}|\psi_1|^4 + \alpha_2|\psi_2|^2 + \frac{\beta_2}{2}|\psi_2|^4 + \text{const}, \quad (23)$$

with both $\alpha_1 < 0$ and $\alpha_2 < 0$. Here F_p is independent of $\theta_1 - \theta_2$ and its minimum occurs at $|\psi_a| = u_a$ where

$$u_a = \sqrt{\frac{-\alpha_a}{\beta_a}}. \quad (24)$$

The Hessian matrix of F_p at $(u_1,u_2,0)$ is

$$\mathcal{H} = \begin{pmatrix} -4\alpha_1 & 0 \\ 0 & -4\alpha_2 \end{pmatrix} \quad (25)$$

whose eigenvalues are $\mu_a^2 = -4\alpha_a$, with corresponding eigenvectors $v_1 = (1,0)^T$, $v_2 = (0,1)^T$. Hence the mixing angle is $\Theta = 0$, the penetration depth is

$$\lambda \equiv \frac{1}{\mu_A} = e^{-1}\left(\frac{-\alpha_1}{\beta_1} + \frac{-\alpha_2}{\beta_2}\right)^{-1/2} \quad (26)$$

and the density decay lengths are the usual coherence lengths

$$\xi_a \equiv \frac{1}{\mu_a} = \frac{1}{2\sqrt{-\alpha_a}}. \quad (27)$$

The criterion for long-range vortex attraction therefore amounts to the requirement that one of the coherence lengths is larger than the magnetic-field penetration length,

$$\min\{2\sqrt{-\alpha_1}, 2\sqrt{-\alpha_2}\} < e\sqrt{\frac{-\alpha_1}{\beta_1} + \frac{-\alpha_2}{\beta_2}}. \quad (28)$$

Note that this criterion indicates only a long-range attraction. For a realization of the type-1.5 regime one should additionally require short-range repulsion and thermodynamic stability of a vortex cluster (i.e., a vortex cluster should become energetically favorable to form in external fields smaller than the thermodynamical critical magnetic field).

Note also that, in systems with independently conserved condensates, such GL models arise from expansion of the free energy in powers $(1 - T/T_{c1})$ and $(1 - T/T_{c2})$ near two critical temperatures (such systems are for example the projected superconducting states of metallic hydrogen or condensate mixtures in neutron stars). In general, T_{c1} and T_{c2} can be quite different, making two such expansions at the same temperature formally impossible. In that case the more suitable model is a London model for one component (i.e., $|\psi_1| \approx$ const except a core cutoff) coupled to a GL model of the second component. When it is the component with "short" coherence length that is modeled by the London limit, we recover a description of the type-1.5 behavior in that case from our above analysis as a simple limit.

B. Josephson coupling

We next consider how this picture is influenced by the addition of an interband Josephson term that breaks the U(1) × U(1) symmetry to U(1),

$$F_p = \hat{F}_p - \eta_1|\psi_1||\psi_2|\cos(\theta_1 - \theta_2), \quad (29)$$

where $\hat{F}_p$ is the free energy defined in Eq. (23) and $\eta_1 > 0$, so that F_p is minimized when $\theta_1 - \theta_2 = 0$. Adding this term changes the vacuum expectation values u_a of the fields. To find u_1,u_2 we must solve

$$\frac{\partial F_p}{\partial|\psi_1|} = \frac{\partial F_p}{\partial|\psi_2|} = 0, \quad (30)$$

that is,

$$2\alpha_1 u_1 + 2\beta_1 u_1^2 = \eta_1 u_2, \quad (31)$$

$$2\alpha_2 u_2 + 2\beta_2 u_2^2 = \eta_1 u_1. \quad (32)$$

Unfortunately, it is not possible to solve these equations explicitly, except in special cases. For particular values of the parameters α_a,β_a,η_1 they can easily be solved numerically, as can the eigenvalue problem for $\mathcal{H}$. Note that like in the case of uncoupled bands, there are in general three fundamental length scales also in the presence of the Josephson term, which can then be computed. We present numerical analysis of this problem in the full Ginzburg-Landau model in Sec. IV. To make analytical advance in this section we treat the η_1

dependence of the length scales perturbatively. That is, we will construct Taylor expansions for $u_a(\eta_1)$, $\mu_A(\eta_1)$, $\mu_a(\eta_1)$, and $\Theta(\eta_1)$. To keep the presentation simple, we will work to order η_1^1, so the results will give the leading correction to the formulas of the previous section as the Josephson coupling η_1 is "turned on." Higher-order corrections are easily computed but do not give much extra insight.

Let us denote quantities defined in the uncoupled model (at $\eta_1 = 0$) with a hat, so $\hat{u}_a = \sqrt{-\alpha_a/\beta_a}$ are the uncoupled vacuum expectation values of $|\psi_a|$, for example. Let $u(\eta_1) = \mathbf{(}u_1(\eta_1),u_2(\eta_1)\mathbf{)}^T$ and

$$G(|\psi_1|,|\psi_2|) = \begin{pmatrix} \partial F_p/\partial|\psi_1| \\ \partial F_p/\partial|\psi_2| \end{pmatrix}. \tag{33}$$

Then, by definition $G[u(\eta_1)] = 0$ for all η_1, and $\hat{G}(\hat{u}) = 0$. Differentiating with respect to η_1 (denoted by a prime), we see that

$$\begin{aligned} 0 &= \frac{\partial G}{\partial \eta_1}(\hat{u}) + \hat{\mathcal{H}}u'(0) \Rightarrow u'(0) = -\hat{\mathcal{H}}^{-1}\frac{\partial G}{\partial \eta_1}(\hat{u}) \\ &= -\begin{pmatrix} \hat{\mu}_1^{-2} & 0 \\ 0 & \hat{\mu}_2^{-2} \end{pmatrix}\begin{pmatrix} -\hat{u}_2 \\ -\hat{u}_1 \end{pmatrix}. \end{aligned} \tag{34}$$

Hence the ground state densities receive a correction linear in η_1,

$$\begin{aligned} u_1(\eta_1) &= \hat{u}_1 + \frac{\hat{u}_2}{\hat{\mu}_1^2}\eta_1 + O\big(\eta_1^2\big), \\ u_2(\eta_1) &= \hat{u}_2 + \frac{\hat{u}_1}{\hat{\mu}_2^2}\eta_1 + O\big(\eta_1^2\big). \end{aligned} \tag{35}$$

From this expression for ground-state densities one can readily calculate the gauge field mass $\mu_A(\eta_1)$, whose inverse gives the London penetration length. One sees that

$$\mu_A(\eta_1)^2 = \hat{\mu}_A^2 + 2\hat{u}_1\hat{u}_2\left(\frac{1}{\hat{\mu}_1^2} + \frac{1}{\hat{\mu}_2^2}\right)\eta_1 + O\big(\eta_1^2\big). \tag{36}$$

So the effect of the Josephson coupling is always to increase the vacuum expectation values of $|\psi_a|$, and hence to decrease the penetration depth $1/\mu_A$.

The other two length scales are the eigenvalues of $\mathcal{H}$ where

$$\begin{aligned} \mathcal{H}_{ab} &= \frac{\partial^2}{\partial|\psi_a|\partial|\psi_b|}(\hat{F}_p - \eta_1|\psi_1||\psi_2|)\Big|_{u(\eta_1)} \\ &= \hat{\mathcal{H}}_{ab} + \eta_1\frac{\partial^3\hat{F}_p}{\partial|\psi_a|\partial|\psi_b|\partial|\psi_c|}\Big|_{\hat{u}}u'_c(0) \\ &\quad - \eta_1(1-\delta_{ab}) + O\big(\eta_1^2\big). \end{aligned} \tag{37}$$

Now

$$\frac{\partial^3\hat{F}_p}{\partial|\psi_a|\partial|\psi_b|\partial|\psi_c|} = \begin{cases} 12\beta_a|\psi_a| & \text{if} \quad a=b=c \\ 0 & \text{otherwise} \end{cases} \tag{38}$$

so

$$\begin{aligned} \mathcal{H} &= \hat{\mathcal{H}} + \eta_1\begin{pmatrix} 12\beta_1\hat{u}_1u'_1(0) & -1 \\ -1 & 12\beta_2\hat{u}_2u'_2(0) \end{pmatrix} + O\big(\eta_1^2\big) \\ &= \begin{pmatrix} \hat{\mu}_1^2 + 3\eta_1\hat{u}_2/\hat{u}_1 & -\eta_1 \\ -\eta_1 & \hat{\mu}_2^2 + 3\eta_1\hat{u}_1/\hat{u}_2 \end{pmatrix} + O\big(\eta_1^2\big). \end{aligned} \tag{39}$$

So the eigenvalues $\lambda = \mu_a^2$ satisfy the characteristic equation

$$\left(\hat{\mu}_1^2 + 3\eta_1\frac{\hat{u}_2}{\hat{u}_1} - \lambda\right)\left(\hat{\mu}_2^2 + 3\eta_1\frac{\hat{u}_1}{\hat{u}_2} - \lambda\right) + O\big(\eta_1^2\big) = 0. \tag{40}$$

Hence

$$\begin{aligned} \mu_1^2 &= \hat{\mu}_1^2 + 3\eta_1\frac{\hat{u}_2}{\hat{u}_1} + O\big(\eta_1^2\big), \\ \mu_2^2 &= \hat{\mu}_2^2 + 3\eta_1\frac{\hat{u}_1}{\hat{u}_2} + O\big(\eta_1^2\big). \end{aligned} \tag{41}$$

As with the penetration depth, the effect of Josephson coupling (at leading order), is to *decrease* the characteristic length scales $1/\mu_a$ of both normal modes. Another effect of Josephson coupling is mixing the fields. Let us now compute the corresponding mixing angle $\Theta(\eta_1)$. Recall that this is, by definition, the angle such that

$$v(\eta_1) = \begin{pmatrix} \cos\Theta(\eta_1) \\ \sin\Theta(\eta_1) \end{pmatrix} \tag{42}$$

is the eigenvector of $\mathcal{H}$ with eigenvalue μ_1^2. We know that $v(0) = \hat{v} = (1,0)^T$, that $v(\eta_1)\cdot v(\eta_1) = 1$, and that

$$M(\eta_1)v(\eta_1) = 0, \quad \text{where} \quad M(\eta_1) = \mathcal{H}(\eta_1) - \mu_1(\eta_1)^2 I_2 \tag{43}$$

for all η_1. As computed above,

$$M(\eta_1) = \begin{pmatrix} 0 & 0 \\ 0 & \hat{\mu}_2^2 - \hat{\mu}_1^2 \end{pmatrix} + \eta_1\begin{pmatrix} 0 & -1 \\ -1 & 3\left(\frac{\hat{u}_1}{\hat{u}_2} - \frac{\hat{u}_2}{\hat{u}_1}\right) \end{pmatrix} + O\big(\eta_1^2\big). \tag{44}$$

Differentiating Eq. (43) and $v(\eta_1)\cdot v(\eta_1) = 1$ with respect to η_1 yields

$$M'(0)\hat{v} + M(0)v'(0) = 0, \quad v(0)\cdot v'(0) = 0, \tag{45}$$

which can be solved for $v'(0)$. One finds that

$$v(\eta_1) = \begin{pmatrix} 1 \\ 0 \end{pmatrix} + \eta_1\big(0\big(\hat{\mu}_2^2 - \hat{\mu}_1^2\big)^{-1}\big) + O\big(\eta_1^2\big). \tag{46}$$

Hence the mixing angle is

$$\Theta(\eta_1) = \frac{\eta_1}{\hat{\mu}_2^2 - \hat{\mu}_1^2} + O\big(\eta_1^2\big). \tag{47}$$

Thus the Josephson term produces mode mixing. Clearly, this perturbative expansion is well defined only if $\hat{\mu}_1 \neq \hat{\mu}_2$. In the case where $\hat{\mu}_1 = \hat{\mu}_2$, $\hat{\mathcal{H}} = \hat{\mu}_1^2\mathbb{I}_2$ and the assertion that $v(0) = (1,0)^T$ is arbitrary, any orthonormal pair of vectors can be taken as the eigenvectors associated with $\hat{\mu}_1^2,\hat{\mu}_2^2$. Hence the notion of "mixing angle" is ill defined in this case, and is not amenable to perturbative calculation.

The normal modes are associated with the following combinations of the $|\psi_a|$ fields:

$$\begin{aligned} \chi_1 &= (|\psi_1| - u_1)\cos\left[\frac{\eta_1}{\hat{\mu}_2^1 - \hat{\mu}_1^2}\right] - (|\psi_2| - u_2)\sin\left[\frac{\eta_1}{\hat{\mu}_2^1 - \hat{\mu}_1^2}\right], \\ \chi_2 &= (|\psi_1| - u_1)\sin\left[\frac{\eta_1}{\hat{\mu}_2^1 - \hat{\mu}_1^2}\right] - (|\psi_2| - u_2)\cos\left[\frac{\eta_1}{\hat{\mu}_2^1 - \hat{\mu}_1^2}\right]. \end{aligned}$$

Thus one can associate "coherence lengths" of these fields with the inverse masses of model (41), which are functions of the coherence lengths ($\hat{\mu}_a^{-1}$) and vacuum field densities ($\hat{u}_a$)

defined in the Josephson-uncoupled theory, and the strength of the Josephson coupling η_1. Note that, returning to the original fields $|\psi_a|$, the very long-range behavior of both of these density fields is governed by whichever of the fields $\chi_{1,2}$ has the slower recovery rate. This implies that at very long range both fields $|\psi_a|$ should have the *same* exponential recovery law set by the smaller of μ_a. The physical meaning of mode mixing is that the variation of the original density fields $|\psi_a|$ acquires two length scales and one should rotate the fields through the mixing angle Θ to determine the normal modes $\chi_{1,2}$ whose recovery rates are governed by different single exponential laws.

Another point to note here is that, from a quantitative point of view, turning on a small Josephson coupling does not radically alter the integer flux vortices. For small η_1, there is a small correction to each of the length scales (all three length scales become smaller), and there is a small amount of normal-mode mixing [measured by $\Theta(\eta_1)$]. Therefore for composite integer flux vortices the addition of Josephson coupling does not represent any kind of singular perturbation.

1. Comparison with the case of passive second band

It is interesting to compare these results with the case where one of the bands, ψ_2 say, is passive, and has superconductivity only by virtue of the Josephson coupling term.[15] In this case, the free energy F_p has $\alpha_2 > 0$. In the uncoupled model (at $\eta_1 = 0$), F_p is minimized when $|\psi_1| = \hat{u}_1 = \sqrt{-\alpha_1/\beta_1}$ and $|\psi_2| = \hat{u}_2 = 0$. The gauge field has mass $\hat{\mu}_A = e\hat{u}_1$, there is no mode mixing, and the condensates have masses $\hat{\mu}_1 = 2\sqrt{-\alpha_1}$ and $\hat{\mu}_2 = \sqrt{2\alpha_2}$. The vortex solution has $\psi_2 = 0$ everywhere and is identical to the Abrikosov vortex of the single-component GL theory with ψ_2 set to zero. As the Josephson coupling is turned on, ψ_2 acquires a vacuum density of order η_1^1, mode mixing develops, and the three length scales acquire corrections. Repeating the arguments of the $\alpha_2 < 0$ case, one finds that

$$\begin{aligned} u_1(\eta_1) &= \hat{u}_1 + O\big(\eta_1^2\big), \quad u_2(\eta_1) = \frac{\hat{u}_1}{\hat{\mu}_2^2}\eta_1 + O\big(\eta_1^2\big), \\ \mu_A(\eta_1)^2 &= \hat{\mu}_A^2 + O\big(\eta_1^2\big), \quad \mu_1(\eta_1)^2 = \hat{\mu}_1^2 + O\big(\eta_1^2\big), \\ \mu_2(\eta_1)^2 &= \hat{\mu}_2^2 + O\big(\eta_1^2\big), \quad \Theta(\eta_1) = \frac{\eta_1}{\hat{\mu}_2^2 - \hat{\mu}_1^2} + O\big(\eta_1^2\big). \end{aligned} \tag{48}$$

A significant difference from the case of two active bands ($\alpha_2 < 0$) is that all three of the length scales receive corrections only at order η_1^2. Nevertheless, there is mode mixing at order η_1^1.

C. Density-density coupling

A similar perturbative analysis of the case when there is biquadratic density-density coupling

$$F_p = \hat{F}_p + \frac{\eta_2}{2}|\psi_1|^2|\psi_2|^2 \tag{49}$$

can be carried out. Since the calculations are similar, we merely record the results (once again, hatted parameters refer to the uncoupled $\eta_2 = 0$ model):

$$\begin{aligned} u_1(\eta_2) &= \hat{u}_1 + \frac{\hat{u}_1\hat{u}_2^2}{\hat{\mu}_1^2}\eta_2 + O\big(\eta_2^2\big), \\ u_2(\eta_2) &= \hat{u}_2 + \frac{\hat{u}_2\hat{u}_1^2}{\hat{\mu}_2^2}\eta_2 + O\big(\eta_2^2\big), \\ \mu_A(\eta_2)^2 &= \hat{\mu}_A^2 + 2\hat{u}_1^2\hat{u}_2^2\left(\frac{1}{\hat{\mu}_1^2} + \frac{1}{\hat{\mu}_2^2}\right)\eta_2 + O\big(\eta_2^2\big), \\ \mu_1(\eta_2)^2 &= \hat{\mu}_1^2 + \left(1 + 3\frac{\hat{u}_2}{\hat{\mu}_1^2}\right)\hat{u}_2^2\eta_2 + O\big(\eta_2^2\big), \\ \mu_2(\eta_2)^2 &= \hat{\mu}_2^2 + \left(1 + 3\frac{\hat{u}_1}{\hat{\mu}_2^2}\right)\hat{u}_1^2\eta_2 + O\big(\eta_2^2\big), \\ \Theta(\eta_2) &= \frac{2\hat{u}_1\hat{u}_2}{\hat{\mu}_1^2 - \hat{\mu}_2^2}\eta_2 + O\big(\eta_2^2\big). \end{aligned} \tag{50}$$

The effect of the extra term is to reduce (if $\eta_2 > 0$) or increase (if $\eta_2 < 0$) all three length scales and to introduce a mode mixing. We present numerical analysis of this kind of coupling in Sec. IV.

D. Mixed gradient terms

In this section we consider the case where the free energy has gradient-gradient coupling terms,

$$\begin{aligned} F = {} & \frac{1}{2}(D_i\psi_1)^* D_i\psi_1 + \frac{1}{2}(D_i\psi_2)^* D_i\psi_2 \\ & - \frac{\nu}{2}[(D_i\psi_1)^* D_i\psi_2 + (D_i\psi_2)^* D_i\psi_1] + F_p, \end{aligned} \tag{51}$$

where $F_p(|\psi_1|,|\psi_2|,\theta_1 - \theta_2)$ is, as before, a non-negative function minimized at $(u_1,u_2,0)$. In contrast to the previous two cases, this we can treat exactly, without resorting to power series expansion in the coupling parameter ν. We can assume $\nu > 0$ without loss of generality (the case $\nu < 0$ is obtained by mapping $\psi_2 \mapsto -\psi_2$), and we must have $\nu < 1$, or else F is not positive definite.

This case does not fit into the general analysis presented above. Nonetheless, a similar method, with some modification, can be applied.

The field equations are

$$D_i D_i(\psi_1 - \nu\psi_2) = 2\frac{\partial F_p}{\partial \psi_1^*}, \tag{52}$$

$$D_i D_i(\psi_2 - \nu\psi_1) = 2\frac{\partial F_p}{\partial \psi_2^*}, \tag{53}$$

$$\begin{aligned} & \partial_i(\partial_i A_j - \partial_j A_i) \\ & \quad = e\,\mathrm{Im}[\psi_1^* D_j(\psi_1 - \nu\psi_2) + \psi_2^* D_j(\psi_2 - \nu\psi_1)], \end{aligned} \tag{54}$$

which support vortex solutions of form (6) provided the profile functions obey the coupled system

$$\begin{aligned} & \left(\frac{d^2}{dr^2} + \frac{1}{r}\frac{d}{dr} - \frac{1}{r^2}(1+ea)^2\right) P \begin{pmatrix} f_1 \\ f_2 \end{pmatrix} \\ & \quad = \begin{pmatrix} \partial F_p/\partial|\psi_1| \\ \partial F_p/\partial|\psi_2| \end{pmatrix}\Bigg|_{(f_1,f_2,0)} \end{aligned}$$

$$a'' - \frac{1}{r}a' - e(1+ea)\big(f_1^2 - 2\nu f_1 f_2 + f_2^2\big) = 0, \tag{55}$$

where

$$P = \begin{pmatrix} 1 & -\nu \\ -\nu & 1 \end{pmatrix}. \tag{56}$$

The vortex boundary conditions are $f_a(r) \to u_a$ and $a(r) \to -1/e$ as $r \to \infty$. Note that these are independent of ν. We again define $\epsilon(r) = \big(f_1(r) - u_1, f_2(r) - u_2\big)^T$ and $\alpha(r) = a(r) + 1/e$, and linearize the system about $\epsilon_1 = \epsilon_2 = \alpha = 0$:

$$\begin{gathered} \left(\frac{d^2}{dr^2} + \frac{1}{r}\frac{d}{dr}\right) P\epsilon = \mathcal{H}\epsilon, \\ \alpha'' - \frac{1}{r}\alpha' - e^2\big(u_1^2 - 2\nu u_1 u_2 + u_2^2\big)\alpha = 0. \end{gathered} \tag{57}$$

We immediately see that $\boldsymbol{A}$ behaves asymptotically as in Eq. (14), but with

$$\mu_A = e\sqrt{u_1^2 - 2\nu u_1 u_2 + u_2^2}. \tag{58}$$

The effect of the gradient-gradient coupling is thus to *increase* the penetration depth $1/\mu_A$. Note that the effect would be opposite if there is a competing sufficiently strong Josephson term which enforces phase *antilocking* in the vacuum, that is, phase difference $\theta_1 - \theta_2 = \pi$.

To decouple the pair of equations for ϵ_1, ϵ_2 we must expand ϵ in a basis of eigenvectors, not of $\mathcal{H}$, but rather of

$$\widetilde{\mathcal{H}}(\nu) = P(\nu)^{-1}\mathcal{H}. \tag{59}$$

Note that this matrix is *not* in general symmetric. Nonetheless, it can be shown that its eigenvalues are real and positive for all $0 \leqslant \nu < 1$ (see Appendix B). Let μ_1^2, μ_2^2 be the eigenvalues of $\widetilde{\mathcal{H}}$ and v_1, v_2 be the corresponding eigenvectors. Then the condensate fields at large r take the form

$$\begin{pmatrix} \psi_1 \\ \psi_2 \end{pmatrix} \sim \left\{ \begin{pmatrix} u_1 \\ u_2 \end{pmatrix} + q_1 K_0(\mu_1 r) v_1 + q_2 K_0(\mu_2 r) v_2 \right\} e^{i\theta}. \tag{60}$$

Once again, the condition for long-range attraction is

$$\min\left\{\mu_1^2, \mu_2^2\right\} < \mu_A^2 \tag{61}$$

but now μ_1^2, μ_2^2 are the eigenvalues of $P(\nu)^{-1}\mathcal{H}$, not $\mathcal{H}$, and μ_A depends on u_1, u_2 and ν, as in Eq. (58). Note that

$$\mu_1^2\mu_2^2 = \det\widetilde{\mathcal{H}} = \det\mathcal{H}/\det P(\eta_1) = \frac{\det\mathcal{H}}{1-\nu^2} \tag{62}$$

so the effect of the coupling must be to increase (at least) one of $\mu_{1,2}$ and hence to decrease (at least) one of the normal-mode recovery length scales. Since $\widetilde{\mathcal{H}}$ is not symmetric, there is no reason why v_1, v_2 should be orthogonal, so it is not possible to define a single mixing angle in this case.

To illustrate, consider the simplest case, where F_p is defined as in Eq. (23). Then $u_a = \sqrt{-\alpha_a/\beta_a}$ and the uncoupled $\nu = 0$ model has $\hat{\mu}_a^2 = -4\alpha_a$ and $\hat{\mu}_A^2 = e^2(u_1^2 + u_2^2)$. For $\nu > 0$, the vacuum expectation values do not change, but the penetration depth increases, since

$$\mu_A^2 = \hat{\mu}_A^2 - 2\nu u_1 u_2. \tag{63}$$

Furthermore,

$$\widetilde{\mathcal{H}}(\nu) = P(\nu)^{-1}\begin{pmatrix} \hat{\mu}_1^2 & 0 \\ 0 & \hat{\mu}_2^2 \end{pmatrix} = \frac{1}{1-\nu^2}\begin{pmatrix} \hat{\mu}_1^2 & \nu\hat{\mu}_2^2 \\ \nu\hat{\mu}_1^2 & \hat{\mu}_2^2 \end{pmatrix} \tag{64}$$

whose eigenvalues are

$$\mu_{1,2}^2(\nu) = \frac{1}{2(1-\nu^2)}\left(\hat{\mu}_1^2 + \hat{\mu}_2^2 \pm \sqrt{\big(\hat{\mu}_1^2 - \hat{\mu}_2^2\big)^2 + 4\nu^2\hat{\mu}_1^2\hat{\mu}_2^2}\right). \tag{65}$$

Now $\mu_{1,2}^{-1}(\nu)$ are the new fundamental length scales which control the variation of the density fields (60). Without loss of generality, we may assume that $\hat{\mu}_1 \geqslant \hat{\mu}_2$ (if $\hat{\mu}_1 < \hat{\mu}_2$ then we simply swap the labels of the condensates). In this case, for $\nu > 0$ it is clear from the above expression that

$$\mu_1^2 > \frac{1}{2(1-\nu^2)}\left(\hat{\mu}_1^2 + \hat{\mu}_2^2 + \sqrt{\big(\hat{\mu}_1^2 - \hat{\mu}_2^2\big)^2}\right) = \frac{\hat{\mu}_1^2}{1-\nu^2} \tag{66}$$

so when $0 < \nu < 1$, $\mu_1(\nu) > \hat{\mu}_1$. Recall that

$$\mu_1^2\mu_2^2 = \det\widetilde{\mathcal{H}} = \frac{\hat{\mu}_1^2\hat{\mu}_2^2}{1-\nu^2}, \tag{67}$$

so

$$\mu_2^2 = \frac{\hat{\mu}_1^2}{\mu_1^2}\frac{\hat{\mu}_2^2}{1-\nu^2} < \hat{\mu}_2^2 \tag{68}$$

by Eq. (66), and hence $\mu_2(\nu) < \hat{\mu}_2$ when $0 < \nu < 1$. In this case, the effect of gradient-gradient coupling is to decrease the smaller of the normal-mode decay lengths, μ_1^{-1}, and increase the larger, μ_2^{-1}. Thus gradient coupling tends to increase the disparity in these length scales.

As in Secs. III B and III C it is instructive to see what happens to the parameters of the uncoupled model ($\nu = 0$) as $\nu > 0$ is turned on. This can be extracted from the above formulas by expanding in ν, keeping only terms up to order ν. One sees that

$$\begin{gathered} u_a(\nu) = \hat{u}_a \quad \text{exactly}, \\ \mu_A(\nu)^2 = \hat{\mu}_A^2 - 2\nu\hat{u}_1\hat{u}_2 \quad \text{exactly}, \\ \mu_a(\nu)^2 = \hat{\mu}_a^2 + O(\nu^2) \end{gathered} \tag{69}$$

so, to leading order in ν, the only length scale that changes is the penetration depth $1/\mu_A$, which increases. The eigenvectors of $\widetilde{\mathcal{H}}$ are

$$v_1 = \begin{pmatrix} 1 \\ \frac{\hat{\mu}_1^2\nu}{\hat{\mu}_1^2 - \hat{\mu}_2^2} \end{pmatrix} + O(\nu^2), \quad v_2 = \begin{pmatrix} \frac{-\hat{\mu}_2^2\nu}{\hat{\mu}_1^2 - \hat{\mu}_2^2} \\ 1 \end{pmatrix} + O(\nu^2), \tag{70}$$

which, one should note, are *not* orthogonal: the angle between them is $\frac{\pi}{2} - \nu + O(\nu^2)$. It follows that the vortex has asymptotic densities (at large r)

$$\begin{aligned} |\psi_1| &\sim \hat{u}_1 + q_1 K_0(\hat{\mu}_1 r) - \frac{q_2\hat{\mu}_2^2\nu}{\hat{\mu}_1^2 - \hat{\mu}_2^2} K_0(\hat{\mu}_2 r) + O(\nu^2), \\ |\psi_2| &\sim \hat{u}_2 + q_2 K_0(\hat{\mu}_2 r) + \frac{q_1\hat{\mu}_1^2\nu}{\hat{\mu}_1^2 - \hat{\mu}_2^2} K_0(\hat{\mu}_1 r) + O(\nu^2), \end{aligned} \tag{71}$$

where q_1, q_2 are unknown constants. So, while the "coherence lengths" remain unchanged to leading order, the normal modes with which they are associated do receive a correction at order ν.

Finally, we remark that an alternative approach to handling gradient-gradient terms is to remove them from F from the outset by a linear redefinition of the fields: essentially one expands $(\psi_1, \psi_2)^T$ in a basis of eigenvectors of $P(\nu)$.[24] This

is mathematically elegant, but tends to obscure the physical meaning of the nongradient terms F_p.

IV. NUMERICAL SOLUTION OF THE NONLINEAR PROBLEM

The linear analysis presented in the previous section can only provide information about the asymptotic tail of the intervortex interaction. To determine the actual full intervortex potential, especially in the case of strong interband coupling, it is necessary to treat the full nonlinear Ginzburg-Landau theory, something which is not possible analytically. In this section we present interaction energies for vortex pairs (including cases of relatively strong interband coupling), computed numerically using a local relaxation method. The numerical method which we use is the following: A lattice approximant of the energy is minimized with respect to all the degrees of freedom in the full Ginzburg-Landau functional subject to the constraint that vortex positions remain fixed. This gives the intervortex interaction energy as a function of intervortex separation. We used high-resolutions grids, with the number of data points ranging from 1600×1600 to 2400×1700, and relaxed each configuration for 50–100 h on an eight-core cluster node.

In this section the length scale is given in units of $2/\hat{\mu}_1$, where, as in Sec. III, $\hat{\mu}_1$ denotes the mass of the field $|\psi_1|$ in the absence of interband couping ($\eta_1 = \eta_2 = \nu = 0$). Alternatively, the unit of length is $\sqrt{2}\hat{\xi}_1$, where $\hat{\xi}_1 = \sqrt{2}/\hat{\mu}_1$ is the coherence length of the first band in the uncoupled case. Recall that $\hat{\xi}_1$ cannot be identified with physical coherence length when interband coupling is present. We also measure condensate density $|\psi_a|$ in units of $\hat{u}_1$, the vacuum expectation value of $|\psi_1|$ in the uncoupled case. As shown in Appendix V, this amounts to using scale freedom to set $\alpha_1 = -1$ and $\beta_1 = 1$. In the single-component limit, the parameter e can then be interpreted as an inverse GL parameter. More precisely, $\kappa = \sqrt{2}/e$, so in these units, in single-component limit, the critical value of e which separates type-I and type-II regimes is $e_c = 2$. The intervortex interaction energy is given in units of total vortex energy, i.e., $2E_v$ where E_v is the energy of a single isolated vortex. All energies are measured relative to the uniform Meissner state ($\psi_a = u_a$, $A = 0$, in the notation of Sec. III).

A. Weak Josephson coupling to a passive band

Let us consider a strongly type-II single-component superconductor, and see how vortex interaction in this system is modified by a weak Josephson coupling to a passive band (i.e., a band which has no superconductivity of its own, which in the context of GL theory manifests itself as a positive coefficient α_2).

Figure 2 shows the vortex interaction energy in such a system. In the limit of decoupled bands, the parameter e is here $e_c/8$. Therefore for zero Josephson coupling this system would have $\kappa \approx 5.7$, putting it far into the type-II region. Weak Josephson coupling changes the length scales as discussed in the previous section and adds a qualitatively new feature: the intervortex potential acquires a minimum, occurring at a separation of approximately $24\sqrt{2}\xi_1$.

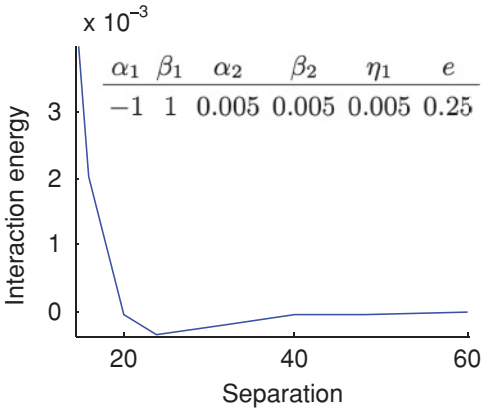

FIG. 2. (Color online) Nonmonotonic vortex interaction in a system with a passive band (i.e., superconductivity is induced in the second band by an intrinsic proximity effect). In the limit of zero Josephson coupling, the active band would have $\kappa = 8\kappa_c$, and thus would be deep into the type-II region. This figure shows that a perturbation in the form of a weak Josephson coupling to passive band in this case produces a minimum in the intervortex potential at a very large distance from the vortex center.

B. Effects of Josephson and mixed gradient terms in case of two active bands

Figure 3 illustrates the effect of the mixed gradient term, as well as of Josephson coupling in a system with two active bands. Curve (4) (green online) corresponds to two independent bands, interacting only through the magnetic field. Curve (2) corresponds to a system with added Josephson coupling, which increases the binding energy, but decreases the distance where the energy minimum is located and slightly reduces the range of interaction.

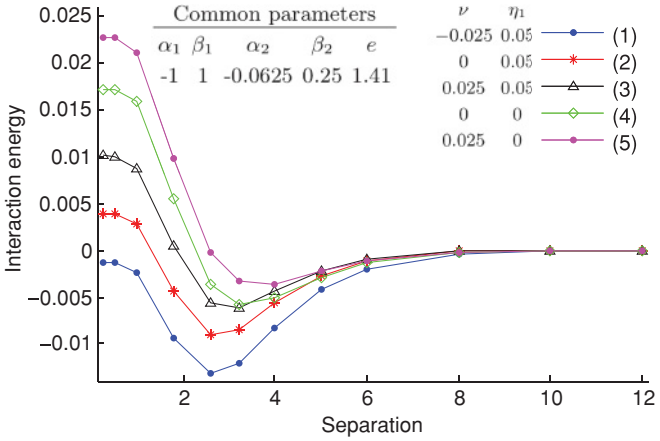

FIG. 3. (Color online) Intervortex interaction potential for a set of systems with two active bands. The systems share the parameters given in the table "common parameters." Curve (4) (green online) corresponds to the case where the bands are coupled by the vector potential only. In this case, the ratio of the coherence lengths is $\xi_2/\xi_1 = 4$. Curve (2) shows the effect of the addition of Josephson term, curve (5) shows the effect of addition of mixed gradient term. Curves (1) and (3) show the effect of the presence of both mixed gradient and Josephson terms with similar and opposite signs.

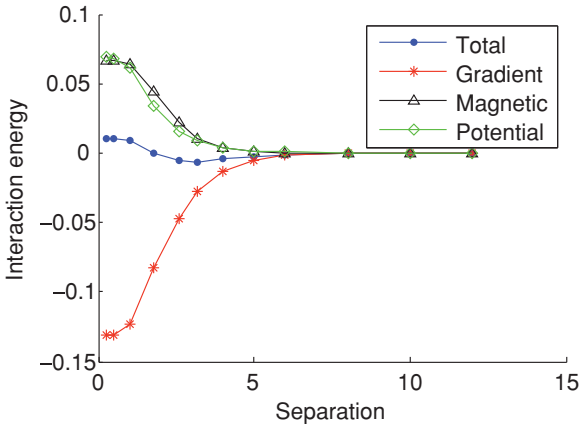

FIG. 4. (Color online) Gradient, magnetic, and potential-energy contributions to the vortex interaction energy for the parameter set corresponding to curve (3) of Fig. 3 (black curve).

The inclusion of a mixed gradient term [shown as curve (5)] here has a similar effect on phase difference as the Josephson term. When the phases are locked $\theta_1 - \theta_2 = 0$, effectively this term gives a negative contribution to the energy associated with co-directed currents. Thus for this choice of the sign of ν, the mixed gradient term also prefers phase locking $\theta_1 - \theta_2 = 0$.

Due to symmetry, changing $\eta_1 \to -\eta_1$ and $\nu \to -\nu$ does not qualitatively change the behavior of the system, as this only results in phase locking with π difference instead. While Josephson coupling increases the energy of vortices, and mixed gradients decreases it, their effect on interaction energy is the opposite. The decomposition of vortex interaction energy into a set of contributions from different terms given in Fig. 4 illustrates why mixed gradients in this case increase repulsion.

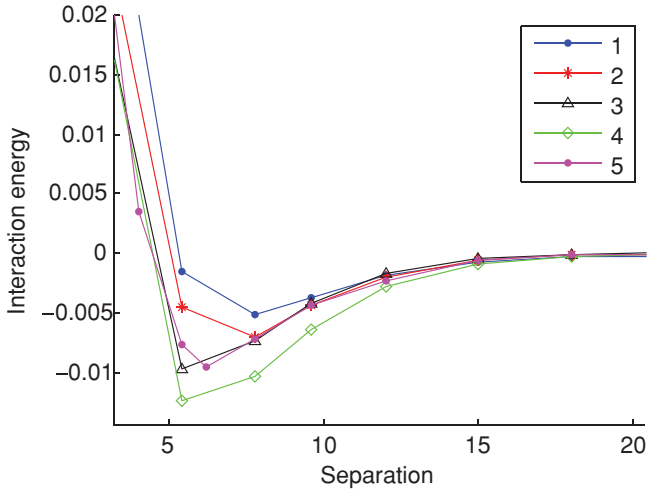

Curve	α_1	β_1	α_2	β_2	η_1	η_2	e	$\langle\lvert\psi_1\rvert^2\rangle$	$\langle\lvert\psi_2\rvert^2\rangle$
1	-1	1	-0.0069	0.0278	0	0	0.7	1	0.25
2	-1	1	-0.0069	0.0278	0.00556	0	0.7	1.0018	0.407
3	-1	1	-0.0069	0.0278	0.0111	0	0.7	1.004	0.526
4	-1	1	-0.0069	0.0139	0	0	0.7	1	0.5
5	-1	1	-0.0069	0.0278	0	-0.0044	0.7	1.00182	0.410

FIG. 5. (Color online) Non monotonic vortex interaction in systems with two active bands and significant disparity in length scales associated with the density variation. In the absence of inter band coupling (curve 1), the ratio of the coherence length is $\xi_2/\xi_1 = 12$.

Curve	α_1	β_1	α_2	β_2	η_1	η_2	e	$\langle\lvert\psi_1\rvert^2\rangle$	$\langle\lvert\psi_2\rvert^2\rangle$
1	-1	1	-0.0069	0.0278	0.0222	0	0.7	1.0094	0.723
2	-1	1	-0.0069	0.0278	0	-0.0077	0.7	1.004	0.526
3	-1	1	-0.0069	0.0278	0	-0.013	0.7	1.0094	0.72
4	-1	1	-0.0069	0.0278	0	-0.0232	0.7	1.026	1.1

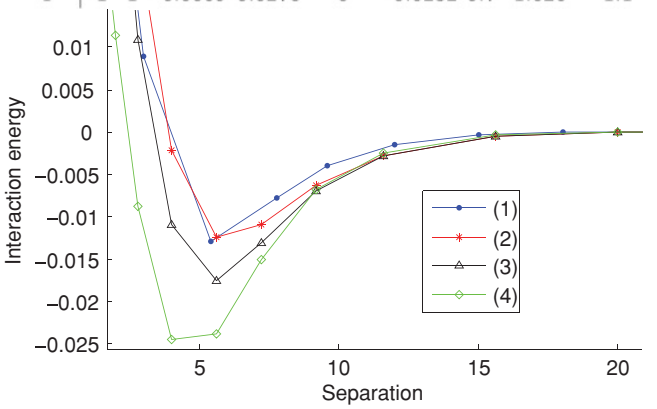

FIG. 6. (Color online) Comparison of how Josephson coupling (1) and high-order density coupling, (2)–(4), affects vortex interaction energy. In (3), η_2 is chosen so that the densities are approximately the same as in (1). In (4), η_2 is chosen to give the same condensation energy as (1). Both these parameter values give larger vortex binding energy. Similar binding energy as (1) is acquired for a significantly smaller η_2 (2). The large condensation energy associated with Josephson coupling is responsible for the shorter interaction range in (1).

In contrast the curve (1) (blue online), corresponds to the case where ν and η_1 have different signs, and so there is competition between the gradient mixing and the Josephson term with regard to the preferred phase difference. The mixed gradient term is minimal for a phase locking where $\theta_1 - \theta_2 = \pi$, while the Josephson term is minimal for $\theta_1 - \theta_2 = 0$. The result in these simulations was that the phase locking was determined by the dominating Josephson coupling, and that the gradient mixing resulted in increased cost for co-directed currents. This was the most energetically expensive vortex, but it also exhibited the smallest intervortex interaction energy.

C. Solutions with large disparity in the characteristic length scales

Figure 5 shows a set of simulations done with two active bands and a larger disparity in characteristic length scales. We start with case when the condensates interact only through the magnetic field [blue curve (1)], and the density in the second band is 1/4 of the density in the first band and the coherence length ratio is $\xi_2/\xi_1 = 12$ (so in the notation of Sec. III, $\hat{u}_1 = 4\hat{u}_2$ and $\hat{\mu}_1 = 12\hat{\mu}_2$). This allows nonmonotonic interaction to occur at smaller e than above—here we simulate at $e = 0.7$. This gives the smallest binding energy in this set of simulations. Adding a Josephson coupling of $\eta_1 = 0.005\,56$ [shown on curve (2)] gives a substantially higher density in the second band, and thus a stronger binding energy. Adding a stronger Josephson coupling [shown on curve (3)] gives even

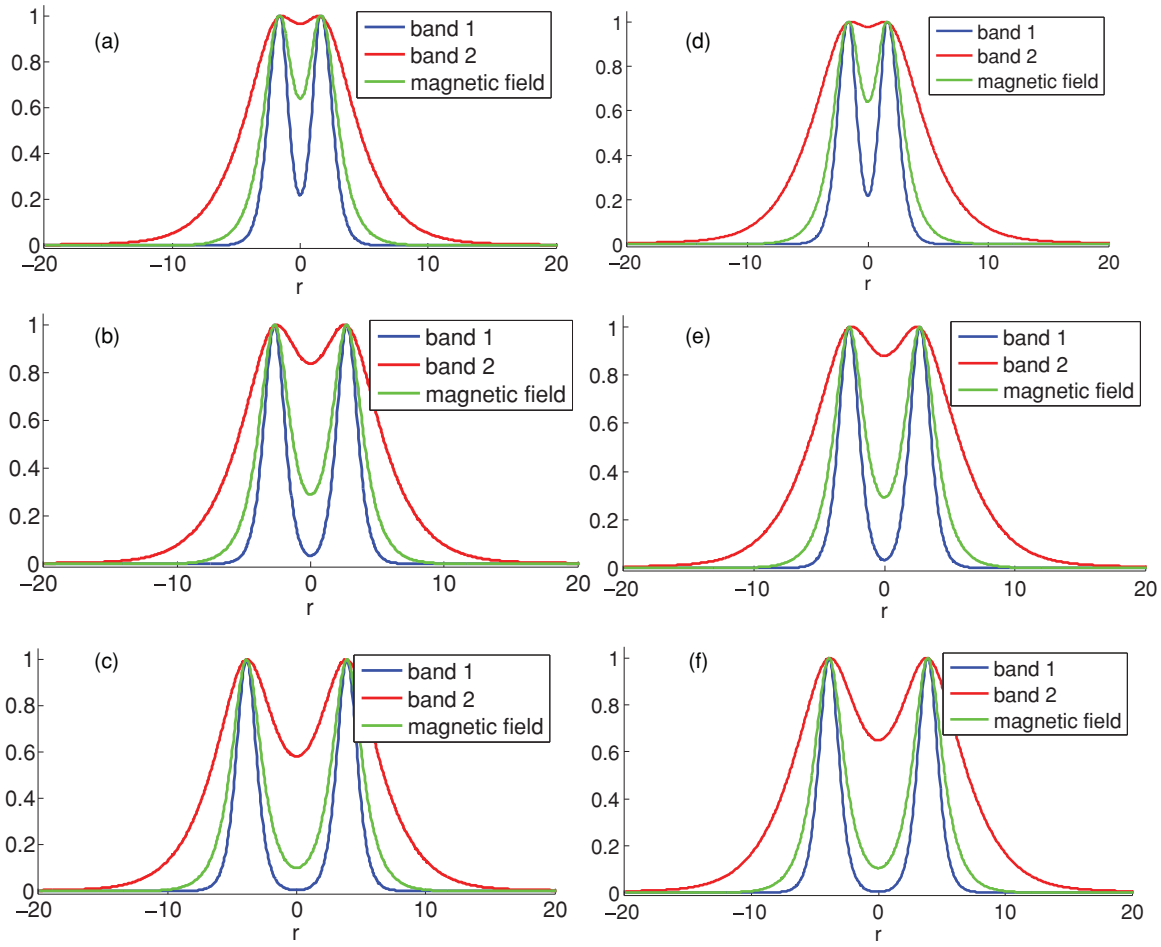

FIG. 7. (Color online) Cross sections of two interacting vortices. The densities are given as $1 - |\psi_i|^2/\langle|\psi|^2\rangle$, i.e., the condensates are normalized to 1 and turned upside down. The magnetic field is also normalized. The left column corresponds to curve (3) of Fig. 5 and the right column corresponds to curve (4) of the same figure. The intervortex separation is 3.0 in the upper row, giving repulsion, 5.4 in the middle row, corresponding to the minimum energy, and 7.8 in the bottom row, giving attraction. Curves 3 and 4 in Fig. 5 are the ones showing the largest binding energy, a property resulting from them having the largest vacuum expectation values in the second band (0.526, 0.5). A careful comparison shows that the recovery of the second band is slower in the right column where there is zero interband coupling. This is a very generic result, Josephson coupling shrinks the disparity in length scales. The result of this effect is also seen when comparing the vortex interaction energies of the two systems, curve (3) reveals a shorter vortex interaction range than curve (4).

larger density in the second band. It also shows some of the qualitative differences associated with this coupling. Namely, the binding occurs at a smaller separation, and the range of the interaction decreases. It is clearly visible that curve (3) crosses the other curves. The Josephson coupling causes the second condensates to recover faster (as follows also from the linear theory presented in the previous section), and thereby decreasing the range of attractive interaction.

Decreasing β_2 raises the density of condensate in the second band. In curve (4), we have reduced it by a factor 2, thereby increasing the vacuum expectation value of the density in the second band by a factor 2. This does, however, not change the length scale, as ξ is independent of β, but it does increase the energetic benefits of core overlap in the second component. This case shows the largest binding energy in this set of simulations.

Finally, we consider the effect of a higher-order density-density coupling η_2 between the condensates, which is shown on curve (5). The parameter choice here gives approximately the same densities as Eq. (2) but smaller condensation energy. This should generally make system (5) recover slower than system (2), resulting in a longer range of the interaction. A more systematic comparison of Josephson coupling and higher-order density coupling supporting this conclusion is given in Fig. 6.

Figure 7 displays cross sections of the condensate densities and magnetic flux in systems (3) and (4) in Fig. 5, clearly illustrating the mechanism by which type-1.5 superconductivity appears.

Let us consider a different example of the appearance of the type-1.5 regime in the case where there is a substantial disparity in the dominant length scales associated with the variations of densities and magnetic-field penetration length.

Again, our starting point is a reference case of two bands coupled only by vector potential where we choose α_2 so that the disparity in coherence length in absence of interband coupling is $\xi_2/\xi_1 = 12$.

Curve	α_1	β_1	α_2	β_2	η_1	η_2	e	$\langle\|\psi_1\|^2\rangle$	$\langle\|\psi_2\|^2\rangle$
1	-1	1	-0.0069	0.0139	0.0055	0	0.5	1.00237	0.73
2	-1	1	-0.0069	0.0139	0.0055	0	0.35	1.00237	0.73
3	-1	1	-0.0069	0.0139	0.0055	0	0.2	1.00237	0.73

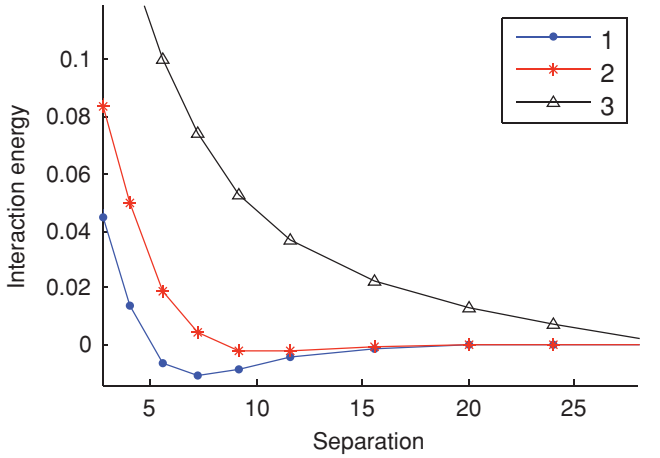

FIG. 8. (Color online) Transition from type-1.5 to type-II region in a system with two active bands. The binding energies are 0.0109 in the first curve and 0.0023 in the second curve. The third curve gives monotonic repulsion. The small binding energy in the second case signals that the critical value for e in this particular example is close to 0.35.

Now, we take β_2 to be 0.0139, i.e., the same as in curve (4) of Fig. 5, and choose the Josephson coupling to be $\eta_1 = 0.005\,56$. Then, we successively decrease e to see where the system crosses over from type 1.5 to type II. The outcome can be seen in Fig. 8. The first curve gives a binding energy of 0.011, the second gives 0.0023, and the third curve shows the system crossing over into the type-II regime by showing monotonic repulsion. Given the small binding energy of the second curve, the crossover from type 1.5 to type II in this example is close to $e = 0.35$.

The cross-section plots of two of these systems given in Fig. 9 illustrate how the system crosses over from type 1.5 to type II as e is decreased, resulting in dominance of the repulsive force originating in the electromagnetic and current-current interaction.

V. CONCLUSIONS

In this paper we presented an analytic and numerical study of the appearance of type-1.5 superconductivity in the case of two bands with various kinds of substantial interband couplings. In all the cases that we considered we demonstrated that the system possessed three fundamental length scales: one length scale $1/\mu_A$, associated with London magnetic-field penetration length, while the other two fundamental scales $1/\mu_{1,2}$ are associated with characteristic length scales controlling variations of density fields. In the limit of two condensates coupled only electromagnetically, the length scales $1/\mu_{1,2}$ are associated with standard coherence lengths. However, we show that introducing a nonzero Josephson and quartic density-density coupling makes both density fields decay according to the same exponential law at very large distances from the core, while at the same time the system still possesses

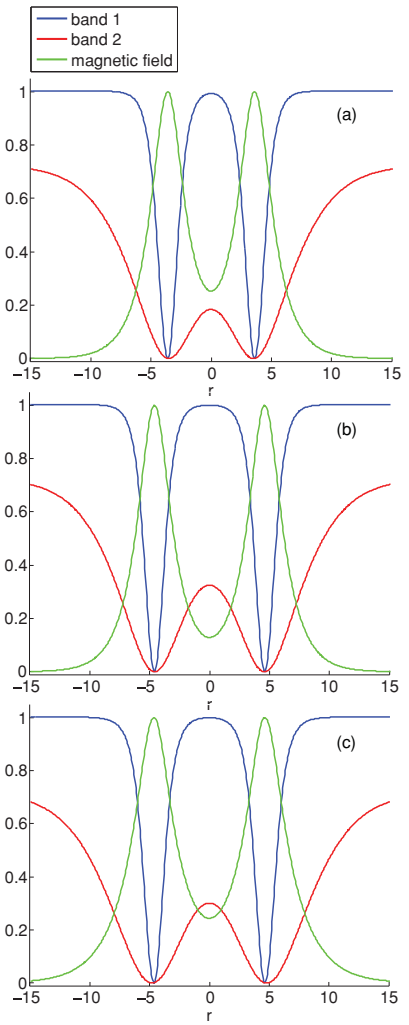

FIG. 9. (Color online) Cross-section plots showing condensate density and magnetic flux in type-1.5 superconductors with small e. (a) Curve (1) in Fig. 8 at a separation of 7.2, corresponding to the energy minimum. (b) The same system at a separation of 9.6. (c) Curve (2) of the same figure at a separation of 9.6, corresponding to the energy minimum. The three distinct length scales associated with two-band superconductors are indeed visible. Despite the interband Josephson coupling, there is a significant disparity in the recovery of the two condensates in all the plots. The third length scale, penetration depth, visibly differs between the two systems, and is responsible for the differences in intervortex interaction.

two fundamental length scales, which are associated now with variation of linear combinations of density fields rotated by a "mixing angle." The third fundamental length scale in that regime is the London penetration length and thus two-band systems with interband couplings allow a well defined type-1.5 behavior. Next we studied the effect of mixed gradient terms and showed how the type-1.5 regime is described in that case. We showed that in the case of a substantial mixed gradient coupling the definition of three fundamental length scales requires additional care because it produces mode mixing that cannot be described by a single mixing angle. Importantly, we demonstrated that mixed gradient coupling can enhance the disparity of the characteristic length scales of the density variations. An analogy can be drawn between this mechanism

and the seesaw mechanism in neutrino physics. In the second part of the paper we presented a comparative numerical study of type-1.5 vortices in the different regimes with various intercomponent couplings. The results were demonstrated in the framework of a two-component Ginzburg-Landau model with local electrodynamics. However, we expect that the described type-1.5 behavior is similarly present in lower-temperature regimes and in two-component models with nonlocal electrodynamics.

The concept of type-1.5 superconductivity can be straightforwardly generalized to N-component case. There it can occur in systems where characteristic length scales are $\xi_1,\ldots,\xi_k < \lambda < \xi_{k+1},\ldots,\xi_N$ and there are thermodynamically stable vortices with nonmonotonic interaction.

Besides multiband superconductors and coexistent electronic and nuclear superconductors, our model can be realized in artificially fabricated layered structures made of type-II and type-I materials where one can control and tune intercomponent Josephson coupling.

It was recently verified in a microscopic calculation, which does not involve $(1-T/T_c)$ expansion, that GL model (2) should quite accurately describe the vortex physics in two-band superconductors in a quite wide range of parameters and temperatures.[25]

ACKNOWLEDGMENTS

We thank Alex Gurevich for discussions. E. B. was supported by Knut and Alice Wallenberg Foundation through the Royal Swedish Academy of Sciences, Swedish Research Council, and by US National Science Foundation CAREER Award No. DMR-0955902. J. C. was supported by the Swedish Research Council. M. S. was supported by the UK Engineering and Physical Sciences Research Council.

APPENDIX A: UNITS

In this Appendix we give an explicit mapping from our representation of the GL model to a more common textbook representation. Consider the Ginzburg-Landau model in the following quite usual units:

$$\begin{aligned}F=&\frac{\hbar^2}{2m_1}\left|\left(\nabla-i\frac{e^*}{\hbar c}A\right)\psi_1\right|^2+\frac{\hbar^2}{2m_2}\left|\left(\nabla-i\frac{e^*}{\hbar c}A\right)\psi_2\right|^2\\&-\nu\hbar^2\mathrm{Re}\left\{\left(\nabla-i\frac{e^*}{\hbar c}A\right)\psi_1\cdot\left(\nabla+i\frac{e^*}{\hbar c}A\right)\psi_2^*\right\}\\&+\frac{1}{8\pi}(\nabla\times A)^2+\alpha_1|\psi_1|^2+\frac{1}{2}\beta_1|\psi_1|^4+\alpha_2|\psi_2|^2\\&+\frac{1}{2}\beta_2|\psi_2|^4-\eta_1|\psi_1||\psi_2|\cos(\theta_1-\theta_2)+\eta_2|\psi_1|^2|\psi_2|^2.\end{aligned}\tag{A1}$$

Let us define the rescaled quantities

$$\widetilde{F}=\frac{4\pi}{\hbar^2c^2}F,\quad \widetilde{A}=-\frac{A}{\hbar c},$$
$$\widetilde{\psi}_a=\sqrt{\frac{4\pi}{m_ac^2}}\psi_a,\quad \widetilde{\nu}=\sqrt{m_1m_2}\nu,$$
$$\widetilde{\alpha}_a=\frac{m_a}{\hbar^2}\alpha_a,\quad \widetilde{\beta}_a=\frac{m_a^2c^2}{4\pi\hbar^2}\beta_a,$$
$$\widetilde{\eta}_1=\frac{\sqrt{m_1m_2}}{\hbar^2}\eta_1,\quad \widetilde{\eta}_2=\frac{m_1m_2c^2}{4\pi\hbar^2}\eta_2.\tag{A2}$$

Then

$$\begin{aligned}\widetilde{F}=&\frac{1}{2}|(\nabla+ie^*\widetilde{A})\widetilde{\psi}_1|^2+\frac{1}{2}|(\nabla+ie^*\widetilde{A})\widetilde{\psi}_2|^2\\&-\widetilde{\nu}\mathrm{Re}\{(\nabla+ie^*\widetilde{A})\widetilde{\psi}_1\cdot(\nabla-ie^*\widetilde{A})\widetilde{\psi}_2^*\}\\&+\frac{1}{2}|\nabla\times\widetilde{A}|^2-\widetilde{\alpha}_1|\widetilde{\psi}_1|^2+\frac{\widetilde{\beta}_1}{2}|\widetilde{\psi}_1|^2+\widetilde{\alpha}_2|\widetilde{\psi}_2|^2\\&+\frac{\widetilde{\beta}_2}{2}|\widetilde{\psi}_2|^2+\widetilde{\eta}_1|\widetilde{\psi}_1||\widetilde{\psi}_2|\cos(\theta_1-\theta_2)+\widetilde{\eta}_2|\widetilde{\psi}_1|^2|\widetilde{\psi}_2|^2,\end{aligned}\tag{A3}$$

which, on dropping the tildes, coincides with representation (2) used in this paper.

Throughout the paper, it is assumed that band 1 is active, that is, $\alpha_1<0$. It is convenient to rescale expression (2) for F further so that α_1 is normalized to -1 and β_1 is normalized to 1. This can be achieved as follows. Recall (see Sec. III A) that in the absence of interband couplings (i.e., when $\eta_1=\eta_2=\nu=0$) condensate 1 has decay length scale $1/\hat{\mu}_1=(-4\alpha_1)^{-1/2}$. This scale is more usually specified by the coherence length

$$\hat{\xi}_1=\frac{\sqrt{2}}{\hat{\mu}_1}=\frac{1}{\sqrt{-2\alpha_1}}.\tag{A4}$$

We emphasize once more that, in the presence of interband couplings, $\hat{\xi}_1$ is not the coherence length of condensate 1. This is the purpose of the hat, to remind us that this is a genuine coherence length only in the uncoupled case. Recall also that the vacuum density of condensate 1 in the uncoupled model is

$$\hat{u}_1=\sqrt{\frac{-\alpha_1}{\beta_1}}.\tag{A5}$$

Our second rescaling amounts to using $\sqrt{2}\hat{\xi}_1$ as the unit of length and $\hat{u}_1$ as the unit of condensate density (along with compensating rescalings of F, e^*, and A). Explicitly, let

$$\begin{aligned}\bar{r}=\frac{r}{\sqrt{2}\hat{\xi}_1}=\sqrt{-\alpha_1}r,\quad \bar{F}=\frac{2\hat{\xi}_1^2}{\hat{u}_1^4}F=\frac{\beta_1^2}{-\alpha_1^3}F,\\ \bar{\psi}_a=\frac{\psi_a}{\hat{u}_1}=\sqrt{\frac{\beta_1}{-\alpha_1}}\psi_a,\quad \bar{A}=\frac{A}{\hat{u}_1},\\ \bar{e}=\frac{1}{\sqrt{2}}\hat{u}_1\hat{\xi}_1e^*=\frac{e^*}{\sqrt{\beta_1}},\quad \bar{\alpha}_2=2\hat{\xi}_1^2\alpha_2=\frac{\alpha_2}{-\alpha_1},\\ \bar{\beta}_2=2\hat{\xi}_1^2\hat{u}_1^2\beta_2=\frac{\beta_2}{\beta_1},\quad \bar{\eta}_1=2\hat{\xi}_1^2\eta_1=\frac{\eta_1}{-\alpha_1},\\ \bar{\eta}_2=2\hat{\xi}_1^2\hat{u}_1^2\eta_2=\frac{\eta_2}{\beta_1},\quad \bar{\nu}=\nu.\end{aligned}\tag{A6}$$

Substituting these into Eq. (2) yields

$$\begin{aligned}\bar{F}=&\frac{1}{2}|(\bar{\nabla}+i\bar{e}\bar{A})\bar{\psi}_1|^2+\frac{1}{2}|(\bar{\nabla}+i\bar{e}\bar{A})\bar{\psi}_2|^2\\&-\bar{\nu}\mathrm{Re}\{(\bar{\nabla}+i\bar{e}\bar{A})\bar{\psi}_1\cdot(\bar{\nabla}-i\bar{e}\bar{A})\bar{\psi}_2^*\}\\&+\frac{1}{2}|\bar{\nabla}\times\bar{A}|^2-|\bar{\psi}_1|^2+\frac{1}{2}|\bar{\psi}_1|^2-\bar{\alpha}_2|\bar{\psi}_2|^2\\&+\frac{\bar{\beta}_2}{2}|\bar{\psi}_2|^2-\bar{\eta}_1|\bar{\psi}_1||\bar{\psi}_2|\cos(\theta_1-\theta_2)+\bar{\eta}_2|\bar{\psi}_1|^2|\bar{\psi}_2|^2.\end{aligned}\tag{A7}$$

This (having dropped the bars) is the GL energy used in Sec. IV for the purposes of numerical simulation.

Finally, we note that the single-component GL model obtained from Eq. (A7) by setting $\psi_2 \equiv 0$ has penetration depth $\lambda = 1/\mu_a = 1/e$ and coherence length $\xi = 1/\sqrt{2}$, and hence GL parameter

$$\kappa = \lambda/\xi = \frac{\sqrt{2}}{e}. \tag{A8}$$

So, in the parametrization used in Sec. IV, one may regard e as an inverse GL parameter for the associated single-band model. The value of e corresponding to the Bogomolny limit of one-component theory is $e_c = 2$ in this interpretation.

APPENDIX B: THE SPECTRUM OF $\widetilde{\mathcal{H}}$

Let $\mathcal{H}$ be a real, symmetric 2×2 matrix, both of whose eigenvalues are positive, and let $\widetilde{\mathcal{H}}(\nu) = P(\nu)^{-1}\mathcal{H}$ where $P(\nu)$ is defined in Eq. (56). We wish to show that the eigenvalues $\lambda_1(\nu),\lambda_2(\nu)$ of $\widetilde{\mathcal{H}}(\nu)$ are also real and positive for all $0 \leqslant \nu < 1$. First note that $\widetilde{\mathcal{H}}(0) = \mathcal{H}$, so the conclusion holds at $\nu = 0$. Further, $\lambda_a(\nu)$ depend continuously on ν. Now $\det\widetilde{\mathcal{H}}(\nu) = \det\mathcal{H}/(1-\nu^2) \neq 0$, so neither eigenvalue ever vanishes. So $\lambda_a(\nu)$ remain real and positive, unless, for some $\nu = \nu_* \in (0,1)$, they coalesce and bifurcate into a complex conjugate pair. But then, at $\nu = \nu_*$ we have $\lambda_1(\nu_*) = \lambda_2(\nu_*) = \lambda_* \in (0,\infty)$ and hence $\widetilde{\mathcal{H}}(\nu_*) = \lambda_* I_2$. But then

$$\widetilde{\mathcal{H}}(\nu) = P(\nu)^{-1}P(\nu_*)\widetilde{\mathcal{H}}(\nu_*) = \lambda_* P(\nu)^{-1}P(\nu_*), \tag{B1}$$

which is symmetric, and hence has real eigenvalues, for all $\nu \in (0,1)$. Hence a bifurcation to a complex conjugate pair of eigenvalues is not possible, and we conclude that $\widetilde{\mathcal{H}}(\nu)$ has real, positive eigenvalues for all $\nu \in [0,1)$.

APPENDIX C: CALCULATION OF LONG-RANGE INTERVORTEX FORCES FROM LINEAR FIELD ASYMPTOTICS

Here we outline how asymptotic intervortex forces are calculated from the linearized asymptotic behavior of the fields. In the above we use a two-component generalization of the method previously developed by one of us in the context of the single-component GL model.[19] The key idea is to identify the vortices with static *topological solitons* in a relativistic extension of the TCGL model to $2+1$-dimensional Minkowski space, which could be called a two-component Abelian-Higgs model. Viewed from afar, the solitons in this theory are identical to the fields induced by suitable point sources in the linearization of the model, so the forces between well-separated solitons approach those between the corresponding fictitious point particles, mediated by linear fields. The nature (attractive or repulsive) and range of such forces can then be computed. In this Appendix we take the opportunity to explain the method in the simplest possible context, with the aim of making it more transparent to a wide readership. Despite being simple and pedagogically motivated, the calculation we present is, as far as we are aware, new, although the result itself has been derived previously by other means.

Consider the sine-Gordon model, which consists of a single scalar field ϕ in $1+1$-dimensional Minkowski space, evolving according to the Euler-Lagrange equation for the action $S = \int \mathcal{L}dt\,dx$ with Lagrangian density

$$\mathcal{L} = \tfrac{1}{2}\partial_\mu\phi\partial^\mu\phi - (1-\cos\phi). \tag{C1}$$

It is useful to think of ϕ as an angular variable, with period 2π, so that the model has a single ground state (or "vacuum"), $\phi = 0$. It also has static kink ϕ_K solutions in which ϕ tends to the vacuum as $x \to \pm\infty$ but winds once anticlockwise. Explicitly,

$$\phi_K(x) = 4\tan^{-1}e^{x-x_0}, \tag{C2}$$

where x_0 is a free parameter. These are topological solitons (topologically stable, spatially localized lumps of energy) analogous to the vortices of the GL model. Their energy density $\mathcal{E} = \frac{1}{2}(\frac{\partial\phi}{\partial x})^2 + (1-\cos\phi)$ is localized in a lump centered at $x = x_0$. At large $|x|$ the kink has asymptotic form

$$\phi_K(x) \sim \begin{cases} 4e^{-|x-x_0|} & x \to -\infty \\ 2\pi - 4e^{-|x-x_0|} & x \to \infty. \end{cases} \tag{C3}$$

We wish to identify this with the field induced by a suitable point source in the linearization of the field theory about the ground state $\phi = 0 \equiv 2\pi$. The linearized field theory has Lagrangian density

$$\mathcal{L}_0 = \tfrac{1}{2}\partial_\mu\phi\partial^\mu\phi - \tfrac{1}{2}\phi^2 \tag{C4}$$

obtained by expanding $\mathcal{L}$ about $\phi = 0$ to quadratic order. The corresponding Euler-Lagrange equation is the Klein-Gordon equation $\phi_{tt} - \phi_{xx} + \phi = 0$ for a scalar field of mass 1, whose general static solution is

$$\phi = c_1 e^x + c_2 e^{-x}. \tag{C5}$$

None of these reproduces the asymptotic kink on the whole real line: one needs $c_2 = 0$ for $x < x_0$ and $c_1 = 0$ for $x > x_0$. To reproduce the kink's asymptotics we must introduce a source term into $\mathcal{L}_0$,

$$\mathcal{L}_0 \mapsto \mathcal{L}_0 + \kappa\phi, \tag{C6}$$

where $\kappa(x)$ is the source. The field equation is now

$$\phi_{tt} - \phi_{xx} + \phi = \kappa(x). \tag{C7}$$

If we take κ to be a scalar monopole of charge q placed at $x = 0$, that is, $\kappa(x) = q\delta(x)$, the induced field is $\phi(x) = \frac{q}{2}e^{-|x|}$. We deduce that the asymptotic kink (C3) will be induced by the point source

$$\kappa_K(x) = m\delta'(x-x_0), \quad m = 8, \tag{C8}$$

which may be interpreted as a scalar dipole of moment m (here δ' denotes the derivative of the δ distribution).

So, viewed from afar, the kink soliton is identical to a scalar dipole in the linear theory. On physical grounds, the interaction energy of a pair of kinks held a fixed distance apart should therefore approach that between a pair of scalar dipoles as the distance grows large. The latter interaction energy is easily computed. Consider the field ϕ induced by a static source $\kappa(x)$ which is itself the sum of two static sources $\kappa_1(x) + \kappa_2(x)$. Since the field theory is linear, $\phi = \phi_1 + \phi_2$, where ϕ_i is the

field induced by κ_i. The total action of the field ϕ and source κ is

$$S = \int \left(\frac{1}{2}\partial_\mu(\phi_1+\phi_2)\partial^\mu(\phi_1+\phi_2) - \frac{1}{2}(\phi_1+\phi_2)^2 + (\kappa_1+\kappa_2)(\phi_1+\phi_2) \right) dx\,dt$$
$$= S_1 + S_2 + \int \kappa_1\phi_2\,dx\,dt, \tag{C9}$$

where S_i is the action of (ϕ_i,κ_i), and we have integrated by parts and used the fact that ϕ_2 satisfies Eq. (C7) with source κ_2. From this we extract the interaction Lagrangian for the pair of sources κ_1,κ_2,

$$L_{\text{int}} = \int \kappa_1\phi_2\,dx. \tag{C10}$$

The case of interest is where κ_i are scalar dipole sources of moment m_i located at x_i. One then has $\kappa_1(x) = m_1\delta'(x-x_1)$ and $\phi_2(x) = \frac{1}{2}m_2\frac{d}{dx}e^{-|x-x_2|}$, and so

$$L_{\text{int}} = \int m_1\delta'(x-x_1)\phi_2(x)\,dx = -m_1\left.\frac{d\psi_2}{dx}\right|_{x=x_1}$$
$$= -\frac{1}{2}m_1m_2e^{-|x_1-x_2|}. \tag{C11}$$

Since the interaction Lagrangian depends only on the dipoles' positions, we can identify $-L_{\text{int}}$ as the interaction potential,

$$V_{\text{int}} = \tfrac{1}{2}m_1m_2e^{-|x_1-x_2|}. \tag{C12}$$

From this we see that like scalar dipoles (m_1,m_2 same sign) repel one another, while unlike dipoles (m_1,m_2 opposite signs) attract. In the case of kinks, $m_1 = m_2 = 8$, so

$$V_{KK} = 32e^{-|x_1-x_2|}, \tag{C13}$$

in exact agreement with a formula of Perring and Skyrme, which they found using a direct superposition ansatz.[26] Kink-antikink interactions can also be recovered from Eq. (C12). Since the antikink is just a reflected kink, $\phi_{\bar{K}}(x) = \phi_K(-x)$, it coincides asymptotically with the field induced by a dipole of moment $m = -8$, so $V_{K\bar{K}} = -32e^{-|x_1-x_2|}$, again in agreement with Perring and Skyrme. So well-separated kinks repel one another, while kinks and antikinks attract one another.

The same basic method works for vortices in the TCGL model, though the details are more complicated. One must linearize the TCGL model about the ground state in real ψ_1 gauge, but now there are three fields rather than one, A, ψ_1 and ψ_2, and ψ_1,ψ_2 are (generically) directly coupled. The coupling is removed by expanding ψ_1,ψ_2 in a basis of normal modes (eigenvectors of the Hessian of the potential). The linearized theory is then identified with a pair of uncoupled Klein-Gordon models and a Proca (massive vector boson) model for A. The point source reproducing the asymptotic vortex is a composite with scalar monopole charges for the two Klein-Gordon fields and a dipole moment for the vector field A. The total interaction energy for a pair of point vortices is the sum of three terms, two attractive (the scalar monopole interactions) and one repulsive (the vector dipole interaction), which can be read off from the quadratic terms in the linear theory's Lagrangian density, as described in Sec. III.

[1] A. Abrikosov, Sov. Phys. JETP **5**, 1174 (1957).

[2] L. Landau, Nature (London) **141**, 688 (1938); R. P. Huebener, *Magnetic Flux Structures of Superconductors*, 2nd ed. (Springer-Verlag, New York, 2001); R. Prozorov, A. F. Fidler, J. Hoberg, and P. C. Canfield, Nat. Phys. **4**, 327 (2008).

[3] The noninteracting regime, which is frequently called "Bogomolny limit" is a property of the Ginzburg-Landau model where, at $\kappa = 1/\sqrt{2}$, the core-core attractive interaction between vortices exactly cancels the current-current repulsive interaction. However, in a realistic system extremely close to the $\kappa \to 1/\sqrt{2}$ limit one should go beyond the Ginzburg-Landau description to determine leftover intervortex interactions, because these are then determined not by the fundamental length scales of the GL theory but by small microscopic effects leading to nonuniversal weak vortex interaction potentials. We do not consider the physics which arises in the Bogomolny limits in this work.

[4] H. Suhl, B. T. Matthias, and L. R. Walker, Phys. Rev. Lett. **3**, 552 (1959).

[5] A. Y. Liu, I. I. Mazin, and J. Kortus, Phys. Rev. Lett. **87**, 087005 (2001); I. I. Mazin, O. K. Andersen, O. Jepsen, O. V. Dolgov, J. Kortus, A. A. Golubov, A. B. Kuzmenko, and D. van der Marel, Phys. Rev. Lett. **89**, 107002 (2002).

[6] A. Gurevich, Phys. Rev. B **67**, 184515 (2003).

[7] A. Gurevich, Physica C **456**, 160 (2007).

[8] M. E. Zhitomirsky and V.-H. Dao, Phys. Rev. B **69**, 054508 (2004).

[9] See e.g., K. Ishida, Y. Nakai, and H. Hosono, J. Phys. Soc. Jpn. **78**, 062001 (2009).

[10] N. W. Ashcroft, J. Phys.: Condens. Matter **12**, A129 (2000); Phys. Rev. Lett. **92**, 187002 (2004); K. Moulopoulos and N. W. Ashcroft, *ibid.* **66**, 2915 (1991).

[11] E. Babaev, A. Sudbø, and N. W. Ashcroft, Nature (London) **431**, 666 (2004); E. Smørgrav, J. Smiseth, E. Babaev, and A. Sudbø, Phys. Rev. Lett. **94**, 096401 (2005); E. Babaev, N. W. Ashcroft, Nature Phys. **3**, 530 (2007).

[12] E. V. Herland, E. Babaev, and A. Sudbo, Phys. Rev. B **82**, 134511 (2010).

[13] P. B. Jones, Mon. Not. R. Astron. Soc. **371**, 1327 (2006); E. Babaev, Phys. Rev. Lett. **103**, 231101 (2009).

[14] E. Babaev and M. Speight, Phys. Rev. B **72**, 180502 (2005).

[15] E. Babaev, J. Carlstrom, and M. Speight, Phys. Rev. Lett. **105**, 067003 (2010).

[16] V. Moshchalkov M. Menghini, T. Nishio, Q. H. Chen, A. V. Silhanek, V. H. Dao, L. F. Chibotaru, N. D. Zhigadlo, and J. Karpinski, Phys. Rev. Lett. **102**, 117001 (2009).

[17] T. Nishio, V. H. Dao, Q. Chen, L. F. Chibotaru, K. Kadowaki, and V. V. Moshchalkov, Phys. Rev. B **81**, 020506(R) (2010).

[18] R. Geurts, M. V. Milosevic, and F. M. Peeters, Phys. Rev. B **81**, 214514 (2010); H. Dao, L. F. Chibotaru, T. Nishio, and V. V. Moshchalkov, Phys. Rev. B **83**, 020503 (2011).

[19] J. M. Speight, Phys. Rev. D **55**, 3830 (1997).

[20]In the case of independently conserved condensates there could be entrainment effects [see e.g., A. F. Andreev and E. Bashkin, Sov. Phys. JETP **42**, 164 (1975)] leading to different mixed gradient terms that are quadratic in gradients and quartic in ψ_a, some of the effects of which on vortex physics were considered in E. Babaev, Phys. Rev. B **79**, 104506 (2009), and in Ref. 12.

[21]E. Babaev, Phys. Rev. Lett. **89**, 067001 (2002); E. Babaev, J. Jaykka, and M. Speight, *ibid*. **103**, 237002 (2009); M. A. Silaev, Phys. Rev. B **83**, 144519 (2011).

[22]M. Abramowitz and I. A. Stegun, *Handbook of Mathematical Functions* (Dover, New York, 1972), p. 374.

[23]B. Plohr, J. Math. Phys. **22**, 2184 (1981).

[24]E. Babaev, J. Carlstrom, and J. M. Speight (unpublished).

[25]M. Silaev and E. Babaev, e-print arXiv:1102.5734 (to be published).

[26]J. K. Perring and T. H. R. Skyrme, Nucl. Phys. **31**, 550 (1962).